PERGAMON

Journal of Structural Geology 24 (2002) 1971–1989

JOURNAL OF STRUCTURAL GEOLOGY

www.elsevier.com/locate/jstrugeo

On the relationship between kilometer-scale sheath folds, ductile thrusts and minor structures in the basal high-pressure units of the Cabo Ortegal complex (NW Spain)

Josu Azcárraga[a], Benito Ábalos[b,*], José Ignacio Gil Ibarguchi[c]

[a]*UTEKI S.A. C/ Vitorialanda, 1-Pab. 4., E-01010 Vitoria, Spain*
[b]*Departamento de Geodinámica, Universidad del País Vasco, PO Box 644, E-48080 Bilbao, Spain*
[c]*Departamento de Mineralogía y Petrología, Universidad del País Vasco, PO Box 644, E-48080 Bilbao, Spain*

Received 17 July 2001; accepted 22 January 2002

Abstract

Large sheath folds in the basal high-pressure nappes of the Cabo Ortegal complex are described and a kinematic interpretation provided. The principal penetrative and map structures relate to regional D2 deformation, which produced foliations (S2) bearing mineral and stretching lineations (L2) and several types of folds (a-type, sheath-like and 'folded folds'). The latter structures are subparallel to the trend of the orogen. Their attitude suggests that the units involved shared a common tectonic evolution during progressive ductile deformation of an anisotropic medium. Reconstruction of major geological structures was accomplished through projection of map-scale features onto the ductile flow plane and the plane perpendicular to the ductile flow direction. The structures reconstructed illustrate their development in the deeper structural levels of an orogenic channel subjected to high-pressure metamorphism during the early phases of the Hercynian orogeny in NW Iberia. We argue that orogen-normal tectonic displacements (of up to a few hundreds of kilometers) represent the minor components of the transpression with possibly thousands of kilometers along-strike dextral displacement between the intervening plates (during subduction/collision). © 2002 Elsevier Science Ltd. All rights reserved.

Keywords: Sheath-fold; Ductile thrusts; High-pressure; Transpression; Cabo Ortegal, Spain

1. Introduction

The existence of large-scale sheath folds in nature has been realized relatively recently. Examples have been described so far in medium- to high-grade metamorphic areas in the internal parts of orogens (Mattauer et al., 1983; Hibbard and Karig, 1987; Vollmer, 1988; Goscombe, 1991; Baudin et al., 1993; Shackleton, 1993; Kleinschrodt and Vollmer, 1994; Kelly et al., 2000). These studies suggest that some metamorphic fold-nappes have a remarkable sheath-like form, and that other nappes might also exhibit such geometry. Coaxiality of mineral and stretching lineations with fold axes is conspicuous, and complex folding patterns resulted from a kinematically simple but intense ductile deformation (Passchier and Trouw, 1996).

In structural geology, the principle of similitude established that minor structures display consistent and predictable three-dimensional relationships to major structures and that such features may be used to identify the geometry of larger structures (Sander, 1930; Wilson, 1961). This principle, widely illustrated in academic texts and used in poorly exposed folded areas, has successfully been applied to sheath folds by Alsop and Holdsworth (1999). Comparison of sheath fold outcrops with down-plunge projections demonstrates the application of this principle. Recognition and geometrical interpretation of nappe structures as sheath folds has often required down-plunge projection of map fold patterns in planes normal to the regional lineation. These are complemented with 'down-lineation projection' profiles (Shackleton, 1993). Thus, areas several kilometers across are projected onto structural sections (whose vertical relief is up to 25–30 km; e.g. King, 1986) that provide windows for studying the structural geology of deep orogenic realms.

In this paper we present structural evidence on the occurrence of large-scale sheath folds within the strongly tectonized, basal nappes of the high-pressure allochthon of Cabo Ortegal (NW Spain). Kinematic interpretation is based upon structures whose size ranges from the micro- to the macroscale. They all illustrate structural development in

* Corresponding author. Fax: +34-4-4648500.
E-mail address: gppabvib@lg.ehu.es (B. Ábalos).

0191-8141/02/$ - see front matter © 2002 Elsevier Science Ltd. All rights reserved.
PII: S0191-8141(02)00005-6

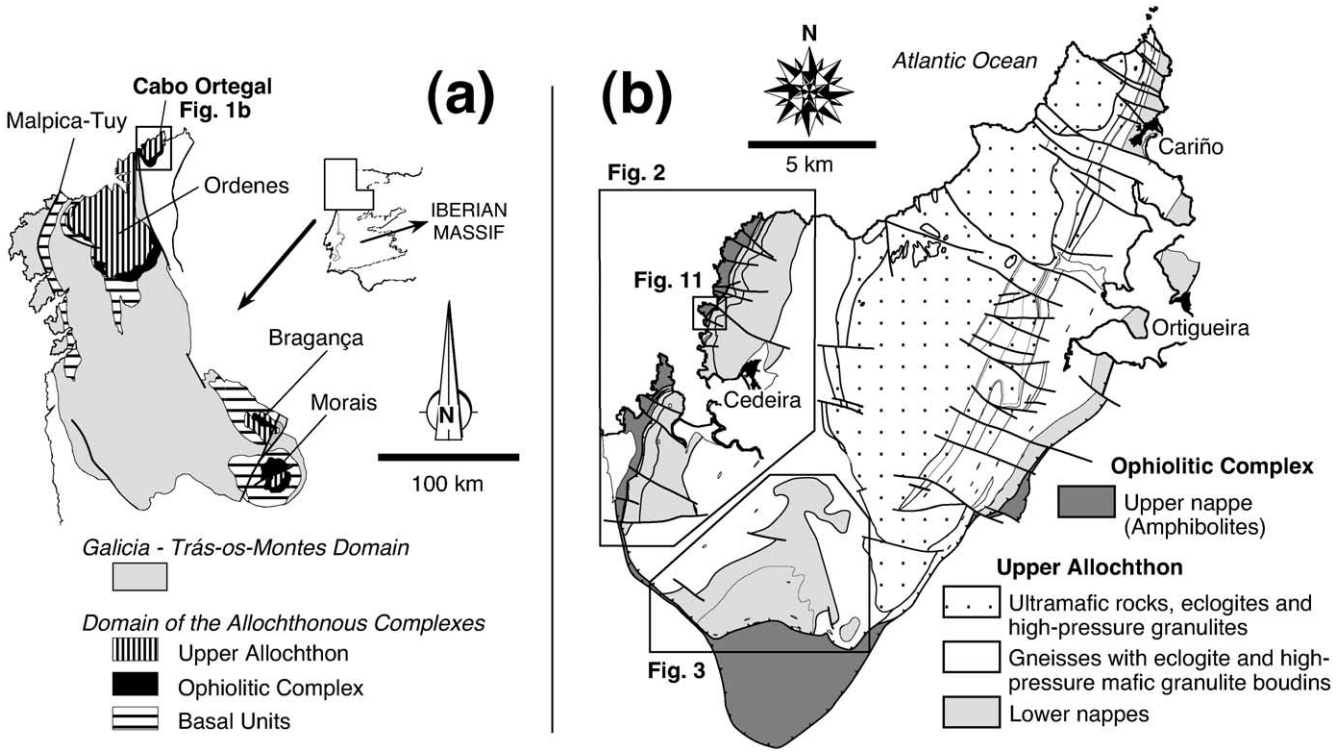

Fig. 1. (a) Geological sketch map of NW Iberia showing the outcrop of the units that constitute the Allochthonous Complexes and their para-autochthon (Domain of Galicia-Trás-os-Montes). (b) Simplified geological map of the Cabo Ortegal complex after Ábalos et al. (2000) showing the internal organization of the high-grade/high-pressure metamorphic nappe units (Upper Allochthon) into (i) an upper ensemble of ultramafic, eclogite and granulite massifs, (ii) an intermediate gneissic group, and (iii) a lower, lithologically heterogeneous, nappe assemblage.

deeper levels of an orogenic channel involving thrusting, folding and penetrative ductile deformation during the early phases of Hercynian subduction/collision in NW Iberia. The term Hercynian refers to the orogenic episode developed between the Upper Devonian and Upper Carboniferous due to the interaction of a number of fragments of continental and oceanic lithosphere between Laurasia and Gondwana. In a broader sense, it is used here to include tectono-thermal events of early Devonian and late Silurian age (for which early Hercynian and eo-Hercynian are also employed).

2. Geological setting

The Cabo Ortegal complex is one of the so-called Allochthonous Complexes of the northwestern Iberian Peninsula (Fig. 1a). These represent fragments of a variably subducted continental and oceanic lithosphere that were subsequently obducted onto the Gondwana edge during the Hercynian orogeny (Ries and Shackleton, 1971; Bard et al., 1980; Iglesias et al., 1983; Peucat et al., 1990; Matte, 1991; Martínez Catalán et al., 1997; Santos Zalduegui et al., 1997).

In the Cabo Ortegal complex (Fig. 1b) crop out parts of the two uppermost structural elements may be recognized and correlated at a regional scale within the Allochthonous Complexes. These are the so-called Ophiolitic Unit at the bottom, and the Upper Allochthon at the top (Martínez Catalán et al., 1997).

The Ophiolitic Unit represents outboard oceanic sequences and delineates the suture zone of the orogen. It consists of thrust sheets of basalts, pillow breccias, diabases, metagabbros, plagiogranites, amphibolites and pervasively serpentinized ultramafic rocks. Higher-grade units are situated in the uppermost structural positions. Metamorphism and continental accretion occurred 390–385 Ma ago (Dallmeyer and Gil Ibarguchi, 1990; Peucat et al., 1990; Dallmeyer et al., 1991), soon after oceanic crust generation 395–Ma ago (Díaz García et al., 1999b).

The Upper Allochthon is represented in Cabo Ortegal by its lowermost units. These are various nappes of high-pressure rocks (high-pressure granulites, N-MORB eclogite, metagabbro, metaserpentinite, metaperidotite and ortho- and paragneisses; cf. Ábalos et al., 1996, and references therein) that can be categorized for descriptive purposes into: (i) an upper ensemble of ultramafic, eclogite and granulite massifs, (ii) an intermediate gneissic group, and (iii) a lower, lithologically heterogeneous, nappe assemblage. The primary structure of the upper and intermediate ensembles relates to earliest, highest-pressure and highest temperature tectonic events (cf. Gil Ibarguchi et al., 1990; Girardeau and Gil Ibarguchi, 1991;

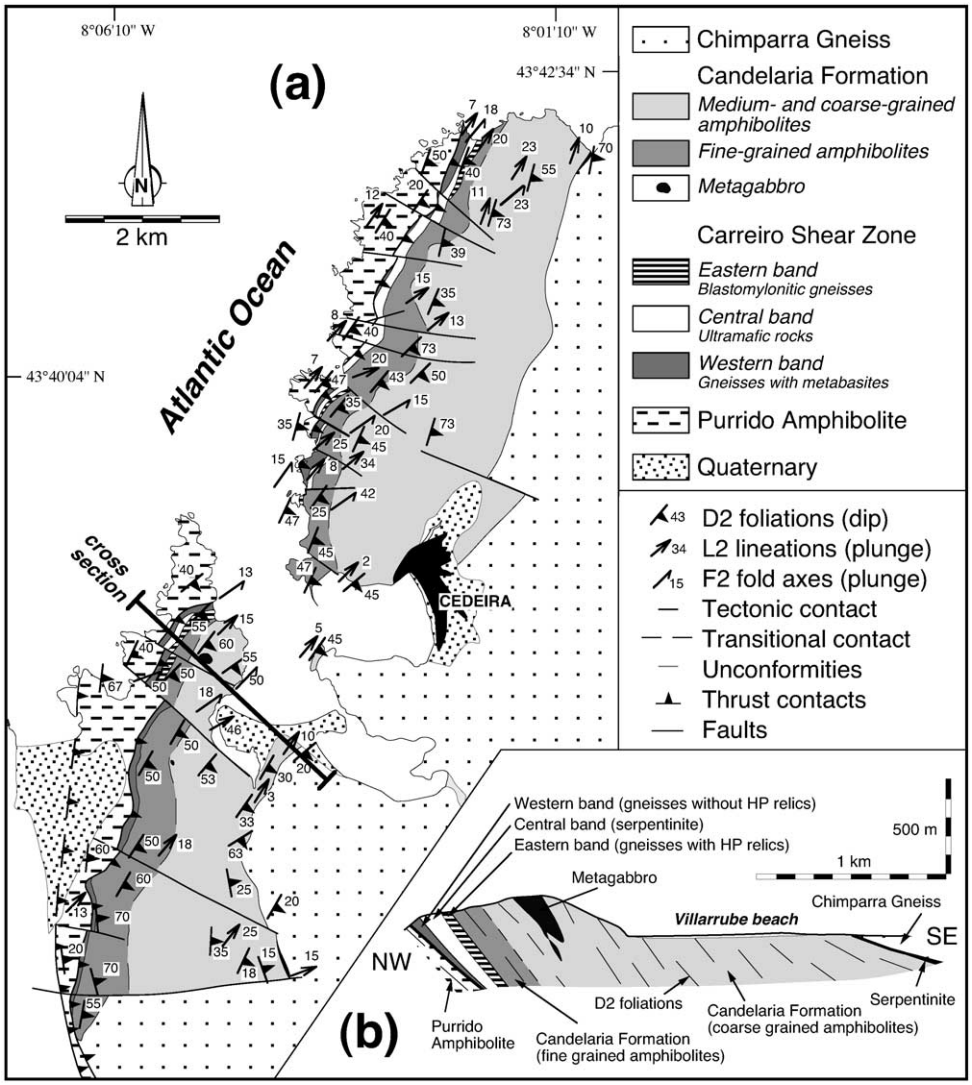

Fig. 2. Geological map (a) and cross-section (b) of the western part of the Cabo Ortegal complex (see Fig. 1b) showing the lithological and structural organization of the lowermost high-grade/high-pressure nappes. The Carreiro Shear Zone (CSZ) conforms to the basal structural zone of this pile. It constitutes a complex and heterogeneous thrust zone with exotic, higher-pressure, upper amphibolite facies hanging wall rocks and lower pressure, amphibolite facies, ophiolitic footwall rocks.

Ábalos et al., 1996; Ábalos, 1997). Precambrian (Ries and Shackleton, 1971; Vogel and Abdel Monem, 1971; Engels et al., 1974), early Paleozoic (Kuijper et al., 1982; Peucat et al., 1990) or middle-late Paleozoic ages (Santos Zalduegui et al., 1996, 2002; Ordóñez et al., 2001) have been proposed for subduction-related high-pressure metamorphism. Amphibolite–facies and later greenschist–facies retrogressions have been estimated at ca. 385 Ma or slightly younger ages (Van Calsteren et al., 1979; Peucat et al., 1990) and between ca. 350 and 360 Ma (Peucat et al., 1990; Dallmeyer et al., 1997), respectively. The principal structural and metamorphic features of the lower nappe ensemble, notably of its basal parts, relate to thrusting of the whole high-grade/high-pressure allochthon onto the Ophiolitic Unit (Marcos et al., 1984; Azcárraga, 1998; Marcos and Farias, 1999).

3. The Upper Allochthon and the Ophiolitic Unit

3.1. The contact zone

The lower nappe ensemble of the upper allochthon is made of various units whose outcrop distribution varies widely. The most complete collages can be found in the western (Fig. 2) and southern parts (Fig. 3) of Cabo Ortegal.

In the western sector (Fig. 2) there may be distinguished, from top to bottom: (i) a thick metabasic unit (Candelaria Formation), (ii) a thin, discontinuous gneissic band containing boudins of high-pressure rocks (Eastern Band), (iii) a discontinuous band of metaserpentinite (Central Band), and (iv) a thin, discontinuous gneissic band lacking high-pressure relics (Western Band). Their contacts are tectonic. The four units are locally in contact with underlying

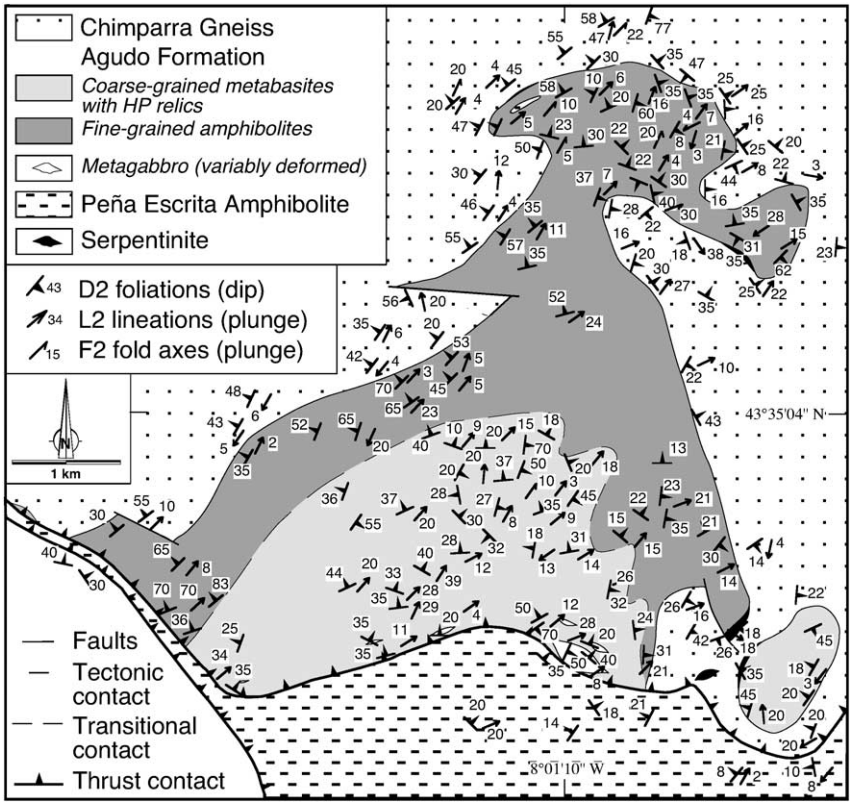

Fig. 3. Geological map of the southern-central part of the Cabo Ortegal complex (see Fig. 1b) showing the lithological and structural organization of the lowermost high-grade/high-pressure nappes. Here, a ductile thrust contact, equivalent to the CSZ, delineates the basal contact of different units (Agudo metabasites and Chimparra gneiss formations) and lower pressure ophiolitic footwall rocks of the Peña Escrita amphibolite. Variably deformed metagabbro intrusions occur along this thrust zone, also. Note that the contacts between the principal units of the high-pressure allochthon are earlier thrusts (cut across by the basal thrust zone) delineated by discontinuous serpentinite slivers.

metabasites (Purrido Amphibolite) that pertain to the Ophiolitic Unit. The term Carreiro Zone of Tectonic Movement (hereafter Carreiro Shear Zone or CSZ) was coined originally by Vogel (1967) to describe a major ductile shear zone in this area of the Cabo Ortegal complex involving lower parts of the Upper Allochthon and uppermost parts of the Ophiolitic Unit (Fig. 2). The ultramafic rocks of the Central Band might delineate the contact between the two major units, though as they contain relics with a high-pressure imprint (Gil Ibarguchi et al., 1999), they are grouped with the Upper Allochthon. In the southern sector (Fig. 3), the contact between the Upper Allochthon (Agudo Formation) and the Ophiolitic Unit (Peña Escrita Amphibolites) is a narrow, ductile shear zone equivalent to the CSZ. The Chimparra Gneiss (that records pressures of >1.6 GPa; cf. Gil Ibarguchi et al., 1987; Fernández, 1994) overlies tectonically both the Candelaria and Agudo Formations, and the Purrido or Peña Escrita Amphibolites (that record similar or lower pressures). The tectonic contact between them is delineated at several places by serpentinite slivers (Vogel, 1967; Ábalos et al., 2000).

In the eastern limb of Cabo Ortegal (Fig. 1b) the boundary between the Upper Allochthon and the Ophiolitic Unit can be traced along the thrust contact between the so-called 'Banded Gneisses' (containing eclogite boudins metamorphosed under 700 °C and >1.6 GPa; cf. Gil Ibarguchi et al., 1987, 1990) and the underlying Cariño Gneisses (lacking high-pressure inclusions and metamorphosed under 650 °C and 0.9 GPa; cf. Basterra et al., 1988; Vielzeuf and Holloway, 1988). Serpentinite slivers also occur along this contact.

3.2. The lower nappes of the Upper Allochthon

The Candelaria Formation is a rather heterogeneous mafic unit up to 1200 m thick. It includes abundant layered amphibolites, variably deformed metagabbro (sometimes coronitic) and calc–silicate rocks (rodingite), metadiabases and metaplagiogranites. Two principal units can be distinguished (Fig. 2) that, probably, denote differences in protolith precursors, deformation intensity and metamorphic grade. On one hand, the 200–500-m-thick western band (occupying the structurally lower position) is composed of fine-grained, mylonitic banded amphibolite. On the other hand, the 800–1200-m-thick eastern band (occupying the structurally upper position) is made of coarse-grained banded amphibolites with abundant relics of gabbro/dolerite and rare garnet–clinopyroxene-bearing rocks.

Coarser-grained amphibolites show a heterogranular texture of blastomylonitic origin. Amphibole, garnet and feldspar porphyroclasts are embedded in an oriented matrix made of feldspar, quartz, amphibole and opaque minerals. Finer-grained amphibolites are pervasively foliated and exhibit a mylonitic microstructure practically devoid of porphyroclasts. High-pressure metabasite relics (made of garnet, clinopyroxene, symplectitic secondary clinopyroxene, amphibole, epidote/clinozoisite, rutile and quartz) exhibit a planolinear tectonic fabric. They record metamorphic conditions transitional between the high-pressure amphibolite and granulite facies (700–800 °C and 0.9–1.3 GPa; cf. Gil Ibarguchi et al., 1990; Hillner, 1995). Later reequilibration during mylonitization occurred at 0.65 GPa and 650–700 °C (Gil Ibarguchi et al., 1987, 1990; Azcárraga, 1998). According to the available geochemical data (Gil Ibarguchi et al., 1990; Peucat et al., 1990), this unit could represent shallower portions of oceanic crust (magma chambers associated with basalt and dyke swarms).

The mafic Agudo Formation consists of a core area with coarser-grained metabasites and a finer grained peripheral area (Fig. 3). The gradual transition between them and the difference in grain size are related to deformation and retrogression intensity. In the core area, variably retrogressed, lensoid high-pressure relics (retrogressed eclogites and granulites that exceptionally preserve igneous textures) are surrounded by bands of garnetiferous amphibolites and metagabbro. Retrogressed eclogites (made of garnet, symplectitic clinopyroxene, quartz, amphibole, epidote/clinozoisite and rutile) exhibit a weak planolinear or linear fabric and a slightly heterogranular texture. The surrounding garnet amphibolites exhibit a planolinear, mylonitic microstructure defined by the dimensional orientation of amphibole, garnet and plagioclase porphyroclasts and aggregates, quartz ribbons, rutile, biotite and titanite/opaque minerals. Though lacking clinopyroxene, they share other petrographic features with the high-pressure relics that point to a similar origin for all these rocks. The exterior envelope is made of medium- to fine-grained, strongly foliated/lineated banded amphibolites and amphibolitic gneisses. They contain garnet- and/or clinopyroxene-bearing lensoid amphibolites comparable with the lensoid high-pressure relics described above. Mappable coronitic metagabbro (Engels, 1972; Azcárraga, 1998) and mylonitic flaser gabbro lenses exist along the basal thrust contact of the unit (Fig. 3).

The Eastern Band of the CSZ (Fig. 2) is up to 40–50 m thick and consists of discontinuous outcrops of garnet–biotite–kyanite–muscovite-bearing mylonitic and blastomylonitic gneisses ('striped gneisses'; Passchier and Trouw, 1996) with high-pressure relics (eclogites, garnet–clinopyroxene metabasites and spinel/garnet peridotite; Gil Ibarguchi et al., 1999). Lenses and layers (decimeter to meter long and sometimes intensely refolded) of the overlying Candelaria amphibolite are common inclusions, also, increasing in abundance towards the hanging wall contact. The latter is delineated by metric- to decametric slices of ultramafic rocks (hornblendite and talc and phlogopite lenses). Peak metamorphic conditions for the gneisses and the eclogite boudins were 800 °C and 1.7 GPa (Azcárraga, 1998). Metaperidotite boudins underwent peak conditions that vary from 900–1050 °C and 1.7–2.0 GPa to 800–900 °C and 2.1–2.4 GPa (Gil Ibarguchi et al., 1999). This was followed by retrogression to 550–570 °C and 8.0–1.3 GPa. The gneisses and their inclusions compare with other mylonitic high-grade gneisses of the complex such as the Chimparra Gneiss and, notably, the much thicker and heterogeneous Banded Gneiss cropping out in a comparable structural position along the eastern area of the complex (Fig. 1b).

The Central Band of the CSZ consists of decameter to hectometer thick and hectometer to kilometer long discontinuous outcrops of strongly serpentinized ultramafites. They are made of chlorite- and chlorite–amphibole schists and exhibit an internal structure depicted by amalgamated, metric to decimetric rock lenses bearing anastomosed foliations and shear zones. The textures and mineral compositions shown by less retrogressed rocks (olivine orthopyroxenite) point to the high-pressure recrystallization of a serpentinite protolith (750–900 °C for a pressure interval of 2.0–3.0 GPa; Gil Ibarguchi et al., 1999).

The Western Band of the CSZ (Fig. 2) contains various types of gneisses made of garnet, biotite, staurolite, kyanite, hornblende, anthophyllite, epidote and rutile. They incorporate metabasite lenses without high-pressure relics (ductilely deformed inclusions of the underlying Purrido amphibolite) that are more frequent towards the footwall contact. Less abundant are calc–silicate, marble, quartz and leucocratic intercalations. The basal contact with the Purrido amphibolite is a meter thick band carrying chlorite- and amphibole-schists. Calculated metamorphic conditions are 650–700 °C and 0.9–1.1 GPa (Azcárraga, 1998). However, the widespread occurrence of rutile, both in the matrix and as inclusions within garnet and other minerals, suggests that earlier metamorphic stages might have attained higher pressures than those calculated. These rocks compare with the Cariño Gneisses of the eastern area of Cabo Ortegal (Fig. 1b).

3.3. The upper nappes of the Ophiolitic Unit

The Purrido and Peña Escrita Amphibolites constitute two connected outcrops in the western (Fig. 2) and southern (Fig. 3) areas of Cabo Ortegal, respectively, bounded by sharp or gradual ductile thrust contacts. Their thickness varies from 650 m to zero. Though some minor petrographic differences exist between them, their geochemical signature (oceanic or back-arc N- to T-MORB; Pin et al., 2000) and metamorphic imprint are similar. The amphibolites are monotonous, penetratively foliated, homogranular, fine- to medium-grained rocks made of hornblende, plagioclase and epidote/clinozoisite. Medium-grained garnet amphibolites and fine-grained leucocratic differentiates are rare.

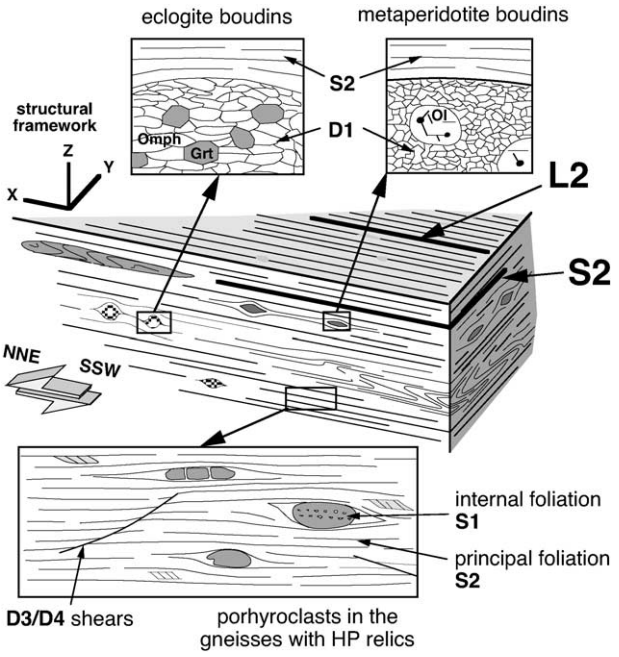

Fig. 4. Sketch diagrams showing the relationships between the principal penetrative structures recognizable in the field and the intervening deformation phases, as deduced from the outcrops of gneisses with high-pressure relics of the eastern gneissic band of the CSZ. Eclogite (Grt, garnet; Omp, omphacite) and metaperidotite boudins (Ol, olivine porphyroclast with spinel inclusions) contain penetrative foliations defined by mineral assemblages with metamorphic grade higher than that of the host gneisses. These and the internal foliations preserved within porphyroclast systems are vestiges of earlier deformations (D1) distinguishable from the principal penetrative structures that define the S2 foliations and L2 mineral and stretching lineations. Discrete, late low-angle shears represent lower-grade deformations ascribable to the D3 and D4 events. See text for further details.

Metagabbro/metadiorite bands sometimes record relic igneous textures. The grain size decreases slightly towards the hanging wall contact. Rutile inclusions in garnet and amphibole document relatively high-pressure early metamorphism prior to amphibolite facies pervasive recrystallization (670 °C, 0.8–0.9 GPa; Azcárraga, 1998) and greenschist–facies dynamic retrogression along shear zones (350–400 °C, 0.25–0.4 GPa; Arenas, 1991).

4. Structural analysis

4.1. Tectonic framework

Based upon microstructural and petrographic criteria, and on the nature and geometrical relationships of penetrative structures, four principal phases of deformation can be recognized (Azcárraga, 1998). D1 is preserved in eclogite and metaperidotite boudins and in relic mineral assemblages surrounded by the main pervasive foliation, which is interpreted to be related to the second deformation phase (D2; see Fig. 4). D1 gave rise to foliations (S1) bearing mineral and stretching lineations (L1) defined by the elongation of crystals and mineral aggregates stable under high-pressure metamorphic conditions (omphacite, olivine, orthopyroxene, etc.). Nappe stacking began during D1 in the uppermost units of the Cabo Ortegal complex, where S1 and L1 are the principal penetrative structures (Gil Ibarguchi et al., 1990; Ábalos, 1997). In the lower nappes, however, the principal penetrative and map structures relate to D2. D2 here produced foliations (S2) bearing mineral and stretching lineations (L2) and several types of folds. S2/L2 are defined by the elongation of minerals stable under relatively high to intermediate pressures and temperatures corresponding to upper amphibolite facies or slightly lower. D2 produced mappable petrographic variations related to ductile deformation in several units (e.g. the grain size modifications of the lower parts of the Candelaria Formation and upper parts of the Agudo Formation). S2 and L2 are geometrically related to principal map structures such as ductile thrusts (the CSZ and its correlatives) and folds. D1 and D2 planolinear fabrics are sometimes concordant, though formed under contrasted metamorphic conditions. D3 and D4 are lower grade syn-metamorphic deformations producing localized foliations and shears that cut across previous structures. They are of minor interest here and will not be described. Later deformations include the development of large (with several kilometer wavelengths), open folds (trending NNE–SSW in the study area). These folds, that tilt and refold all previous structures and contacts, are well known in the regional geological literature (Bastida et al., 1984).

4.2. D2 penetrative structures and folds

The orientation of the main penetrative structures (S2 and L2; Fig. 5a) is similar in the units that constitute the CSZ and in its hanging wall (Upper Allochthon) and footwall (Ophiolitic Unit). Folds of all scales are notable structures of these units that exhibit comparable attitudes in all of them (Fig. 5b). Their profile geometry, the microstructural relationships with the penetrative ductile fabrics, and the attitude of the fold axial surfaces (P2) and fold axes (A2) parallel to the principal foliation (S2) and lineation (L2), respectively, jointly suggest a genetic connection between foliation/lineation and fold development. As folds deform S2, it could be disputed that they correspond to a later tectonic event (e.g. Bastida et al., 1984; Marcos et al., 1984). Here we interpret that folds formed concomitant with the progressive development of foliations and their subsequent heterogeneous ductile deformation, since it is a well known process in ductile shear zones (Passchier and Trouw, 1996; Carreras, 2001).

Folds are common in units of varied lithology (gneissic, metabasic or ultramafic). Folds are often decimetric to metric in size and exhibit isoclinal geometry in profile sections (Fig. 6a and b), with thickened hinges and thinned limbs. There is a striking parallelism between fold axes and L2, and between fold axial surfaces and S2 (Fig. 5). In

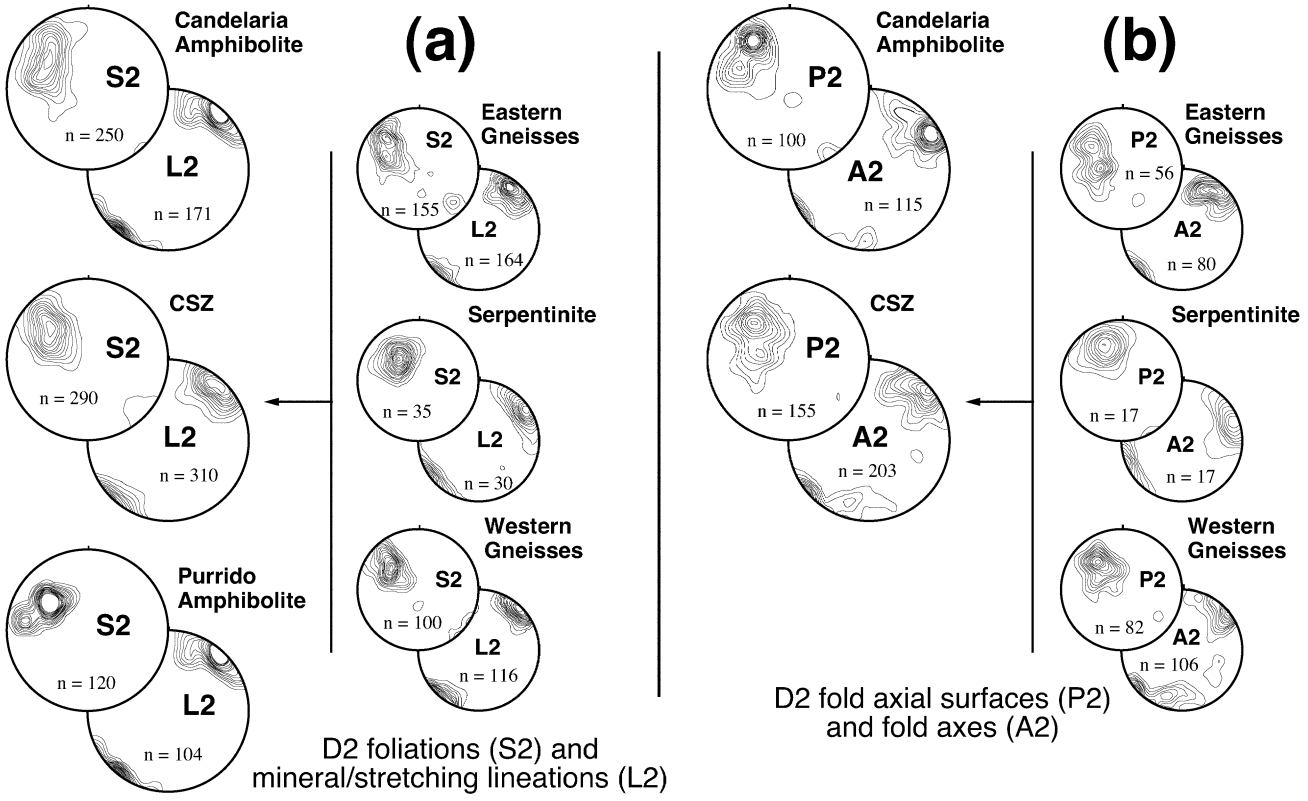

Fig. 5. Equal area, lower-hemisphere stereoplots (contours in multiples of uniform distribution) showing the orientation of: (a) the principal foliation (S2) and lineation (L2), and (b) the axial surfaces (P2) and axes (A2) of the coeval isoclinal folds in the units shown in Fig. 2. CSZ, Carreiro Shear Zone. Note the close orientation relationship across different units between the structural elements represented, the close relationship between the orientation of S2 foliations and P2 axial surfaces and between L2 lineations and A2 fold axes. This suggests a genetic relationship, in addition to the geometrical, between folds and foliations/lineations across a thick shear zone.

outcrop sections normal to S2 that contain L2 (*XZ* structural sections) these folds exhibit isoclinal geometry, too (e.g. Fig. 6a). As regards their three-dimensional geometry, they are often cylindrical folds (a-type folds). However, sheath-type folds (Fig. 6c and d) can also be recognized closely associated with them, notably in shear bands parallel to S2. In structural sections normal to L2 (*YZ* sections) the geometrical patterns of foliations disturbed by sheath folds can be observed (Fig. 6d and e). There, foliations delineate eye-like (closed) subelliptical, anvil (open) and double-vergence fold morphologies. The apical zones and the curved hinges of sheaths can occasionally be observed locally (Fig. 6c). The progressive curvature of the fold hinges enables recognition of geometrical relationships with the mineral/stretching lineations that vary from perpendicularity in the apical zone to parallelism in the limbs. Folding of the principal foliation and the contained lineation leading to the formation of classical sheath fold geometries is a process usually controlled by the presence of metabasic boudins, or favored by a more pronounced mechanical heterogeneity (e.g. alternation of coarser- and finer-grained amphibolite layers). Also in structural sections normal to L2, complex fold geometries that resemble the type-3 fold interference pattern of Ramsay (1967) are common (Fig. 6e and f). In previous studies of Cabo Ortegal, most authors have interpreted these intricate patterns of folding as the result of the superposition of various phases of deformation (Vogel, 1967; Engels, 1972; Arps et al., 1977; Den Tex, 1981; Bastida et al., 1984; Marcos et al., 1984).

In the Purrido–Peña Escrita Amphibolites of the underlying Ophiolitic Unit, D2 folds are rare and small (decimetric) and concentrate along discrete bands near the CSZ. Their principal characteristics are as described above. Bastida et al. (1984) and Marcos et al. (1984) recognized two generations of folds in this unit. Asymmetric intrafolial folds verging toward the East (down-dip) were attributed to a first generation, whereas geometrically equivalent folds verging to the West were ascribed to the second generation. For these authors, folds and foliation development would be related only in the case of the first generation folds. Based upon our field observations, the axes of minor folds with S or Z geometries are parallel to the apical axes of undisputable sheath folds and to mineral/stretching lineations. These relationships at the outcrop scale also occur at larger scales, being similar to those described in detail elsewhere (Vollmer, 1988; Alsop and Holdsworth, 1999). Even in the case of anvil-like, double vergence structures, Goscombe (1991) discussed that these patterns are not the result of fold superposition, but of sheath-folding.

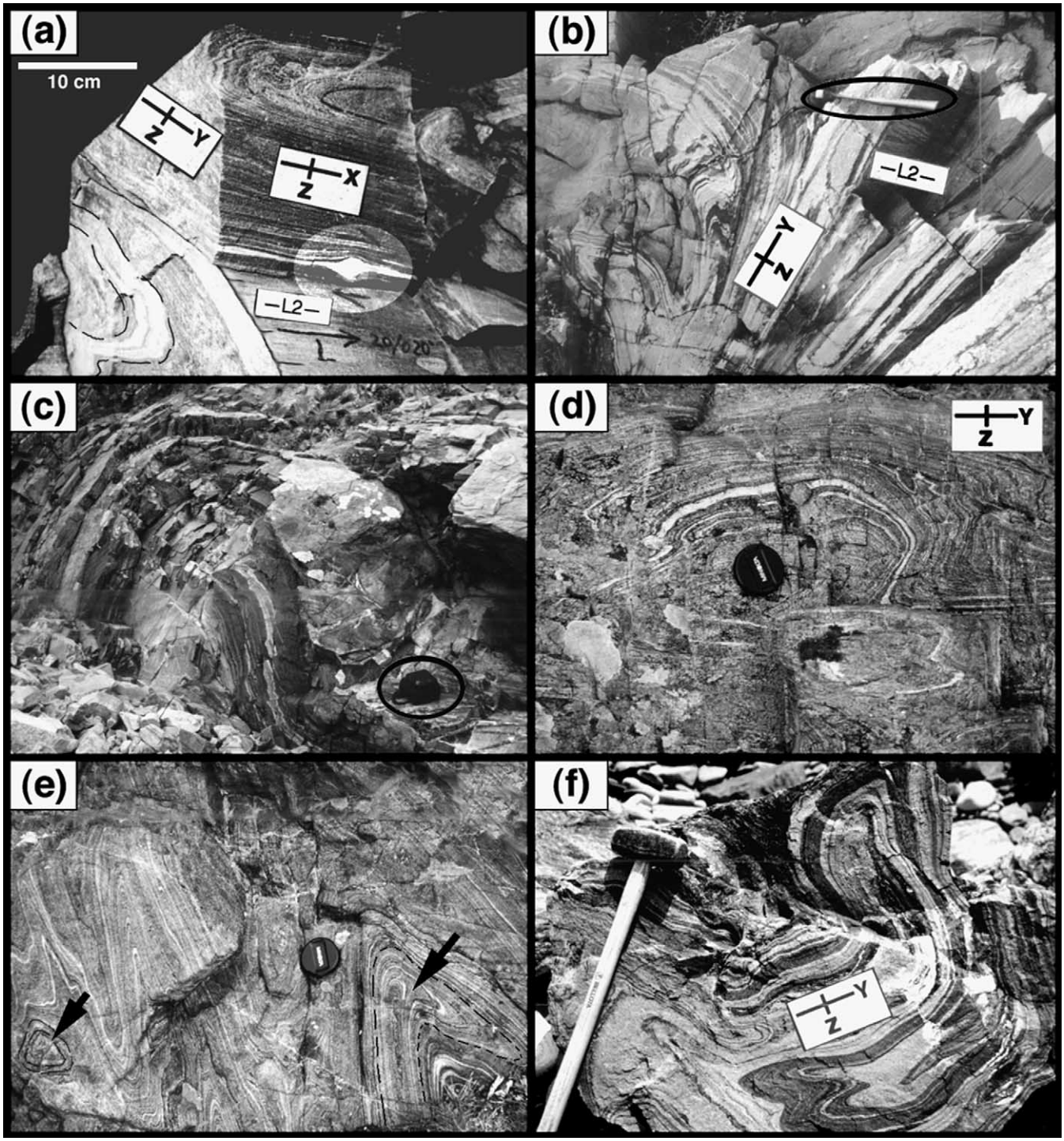

Our structural interpretation of folds (a-type, sheath-like and 'type-3 interference folds') assumes progressive ductile deformation of an anisotropic medium during D2. This process is common in shear zones, where foliations and lineations form and deform, even repeatedly, in the course of single progressive deformation phases. Fold geometries also indicate that S2 accommodated pervasive shear parallel to the direction of L2. In this scheme, S2 and L2 represent the plane and direction of ductile rock flow during D2 syn-metamorphic deformation.

4.3. Microtectonics and kinematics

Kinematic indicators related to D2 are abundant in all the units studied. They include σ-, δ-type and complex stair-stepped porphyroclast systems, C–S and S–C' structures, asymmetric pressure shadows, oblique quartz c-axis fabrics in quartz ribbons, and the asymmetry of sheath folds at the micro- and mesoscale. All these vorticity gages point to the onset of non-coaxial components during D2, and indicate consistently a top-to-the-NE sense of movement of hanging wall blocks.

Unrecrystallized parts of a small proportion of porphyroclast systems appear to indicate the opposite sense of movement or are ambiguous. Taking into account their special internal geometry and their entire association, they can be interpreted according to the scheme of Simpson and De Paor (1993). To determine the degree of non-coaxiallity associated with D2, quantitative estimations of the vorticity number (Wk; Truesdell, 1954) have been performed using the geometry of porphyroclast systems and following the methods of Passchier (1987) and Simpson (1992). The results obtained for Wk using the two methods (Fig. 7) are close to 0.5 (in a range from 0.45 to 0.80), which suggest the operation of general shear.

Further complexity (e.g. the occurrence of symmetric ϕ-type porphyroclasts) can be related to flow instabilities, heterogeneity induced by mechanical anisotropy and differences in the rheology of deforming materials (e.g. power-law creep vs. Newtonian flow, cf. Passchier, 1994). This is highlighted by the analysis of quartz *c*-axis fabrics and determination of differential stresses and strain rates associated with D2 (Azcárraga, 1998). Quartz *c*-axis fabric distributions were measured with a Leitz five-axis U-stage in *XZ* structural sections of deformed quartz veins and ribbons (Fig. 8). Stereoplots show a variety of fabric patterns consistently oblique to the structural reference frame. They contain point maxima and girdles indicative of the operation of quartz intracrystalline slip systems active under medium- to high-grade metamorphic conditions (i.e. prism-⟨a⟩ and prism-[c], active under temperatures $>$ 570 °C; cf. Mainprice et al., 1986), in consonance with prevailing thermobaric conditions of stability of the mineral assemblages defining D2 fabrics. Differential stresses and strain rates (calculated following the method described in further detail by Ábalos et al. (1996)) indicate low differential stress (10 MPa) and slow strain rate deformation (10^{-17}–10^{-14} s^{-1}) of the whole nappe ensemble during early, highest temperature D2 stages. Subsequent deformations occurred under moderate differential stress (30 MPa) and faster strain rates (10^{-13}–10^{-11} s^{-1}) concomitant with deformation localization at decreasing temperature (Azcárraga, 1998). These results also imply that the CSZ and the adjacent units behaved in the course of D2 as a spatially heterogeneous medium composed of relatively undeformed high-viscosity masses separated by intensely deformed low-viscosity channels.

5. Geometry and kinematics of nappe emplacement

5.1. Basis for the structural reconstruction

Structural analysis (geometry and kinematics) of the CSZ and related units in the two areas studied (Figs. 2 and 3) showed that mineral and stretching lineations are parallel to isoclinal fold axes and to the apical axes of sheath folds. Thus, they can be interpreted as tracers of the tectonic transport direction. This direction and the orientation of D2 flow surfaces (foliations) show quite stable attitudes (Figs. 5 and 9a and b) in the two areas. On one hand, in the area of Fig. 2, S2 trends ca. N041°E and dips ca. 40° SE, and bears L2 lineations plunging ca. 11° toward N044°E. On the other hand, in the area of Fig. 3, S2 contains L2 lineations plunging ca. 12° toward N044°E. The attitude of S2 in the latter area is not so stable as in the former due to intense map-scale D2 folding (Fig. 10a). However, L2 bears a rather constant orientation (Fig. 10b) independent of the strike and dip of S2 (Fig. 9c). Additionally, the orientation of L2 coincides with that of the F2 fold axes (Figs. 9a and b and 10b) and also with the orientation of the fold axis that can be deduced from the stereoplots of Figs. 9a and 10a.

The previous geometrical relationships have been taken into consideration for reconstructing structural sections of the contact between the Upper Allochthon and the Ophiolitic Unit along planes parallel and perpendicular to the interpreted direction of ductile rock flow. These sections would enable a better understanding of the structure and kinematics of the CSZ. So far, cross-sections have been constructed in the direction normal to the regional strike of foliations (Fig. 11), providing only limited information on the geometrical and kinematic relationships because of the complex folding patterns.

Fig. 6. Field views of folds developed in different lithotypes of the Carreiro Shear Zone and adjacent units. (a) Outcrop of gneisses with high-pressure relics (eastern band of the CSZ) showing the relationships between folds, foliations, lineations and porphyroclasts systems (highlighted with an ellipse) in three almost perpendicular sections. The bottom section with the label -L2- represents a S2 foliation surface containing straight mineral and stretching lineations that trend 20°/020° (pencilled with a marker). The section in the center is close to a *XZ* structural section and contains both isoclinally folded layers and stair-stepped porphyroclast/ribbon systems indicating unambiguously a top-to-the-NNE sense of movement of the hanging wall. The section to the left represents a structural *YZ* section and exhibits isoclinally folded layers. (b) Outcrop of gneisses from the eastern band of the CSZ showing notably a perspective of complexly folded layers (apparently polyphase isoclinal folds) in a *YZ* structural section, normal to the orientation of gently plunging lineations (labelled -L2-) visible in the central-right part of the photograph, under the encircled hammer. (c) Three-dimensional perspective of a meter-scale sheath fold (note the ellipsed backpack at the bottom right) developed in the western gneissic band of the CSZ. The apical axis of the fold is subhorizontal and points to the right of the observer. The fold is partly dissected. (d) Folded amphibolite of the Candelaria Formation near the CSZ showing closed eye-like and anvil morphologies in an outcrop section perpendicular to the regional L2 lineation (*YZ* structural section). (e) Folded amphibolite of the Candelaria Formation near the CSZ showing apparently polyphase isoclinal folding in an outcrop section perpendicular to the regional L2 lineation (that trends subhorizontal towards the observer). Note the occurrence of closed eye-like forms at the lower left and of folded layers with geometries akin to the Ramsay's (1967) type-3 fold interference pattern at the lower right. (f) Folded gneisses with metabasite layers of the western band of the CSZ in an outcrop section perpendicular to the regional L2 lineation. As in (e), the geometry of the folded layers resembles Ramsay's (1967) type-3 fold interference patterns.

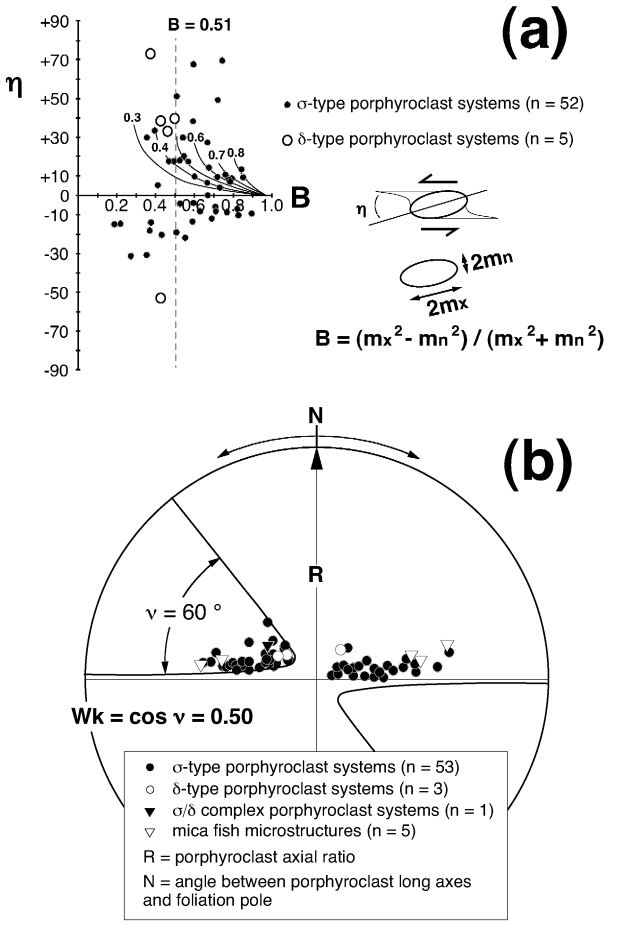

Fig. 7. Determination of the degree of non-coaxiallity of D2 ductile deformation after the geometry of porphyroclast systems in *XZ* structural sections following the methods of: (a) Passchier (1987), and (b) Simpson and De Paor (1993). In (a) 'η' is the angle between the recrystallized tails and the long axis of the unrecrystallized region of the porphyroclast system. The parameter 'B' is a measure of the shape ratio of the unrecrystallized region. The curves drawn in the B–η plot correspond to the theoretical porphyroclast geometries calculated for various non-coaxial deformations whose vorticity number (Wk) is indicated. The dashed line separates the fields of stagnated and rotating porphyroclast orientations. The value of the 'B' parameter is equivalent to the vorticity number Wk there. In (b) the hyperbolic net of De Paor (1988) is used to plot the shape ratio of the porphyroclasts ('R', increasing radially from one in the center of the plot) against the angle 'N' formed between their long axes and the pole to the foliation, both measured in *XZ* sections. The hyperbolic curve with asymptotes forming 69° contains the porphyroclast systems with stable orientations. The cosine of this angle ('ν') gives the vorticity number (here Wk = 0.36) associated with the D2 ductile deformation.

5.2. Section parallel to the flow direction

In Fig. 12a, a structural reconstruction of the CSZ is shown, projected onto a plane perpendicular to the regional S2 and parallel to L2. The orientation of the projection plane (trending N041°E and dipping 50° NW) was determined from eigenvector calculation procedures using the Stereoplot software (Mancktelow, 1990) applied to S2 and L2 field data from the area of Fig. 2. In the new reference frame the principal ductile flow components are contained within the plane of the cross-section. This is highlighted with the stereoplots, for which construction field S2 and L2 data were rotated so that the equatorial section is parallel to the cross-section projection plane, thus representing the relative geometrical disposition of flow planes and flow directions. In this reconstruction a remarkable concordance in S2 and L2 disposition among the different units is observed.

The CSZ appears in this context as a narrow, 200–300-m-thick ductile thrust concentrating the principal of the tectonic displacement between the Upper Allochthon (hanging wall) and the Ophiolitic Unit (footwall). This is interpreted as the result of deformation localization concomitant with temperature decrease and/or increase in the strain rate. Early stages of D2, taking place under upper amphibolite-facies temperature conditions and relatively high pressures, affected the whole thickness of rock units (ca. 2 km). Weak syn-metamorphic cooling or increase in the rate of deformation led in a first stage to strain localization in a band up to 500–700 m thick containing the dynamically recrystallized, fine-grained part of the Candelaria Formation. During this episode strain localization also occurred along the upper contact of the Candelaria Formation with the Chimparra Gneiss, leading to the formation of a thin band of mylonitic, fine-grained amphibolite (not shown in Fig. 2). Further cooling (still in the amphibolite facies) or strain rate increase led to D2 localization in a thin channel, the CSZ, at the base of the Candelaria Formation. D2 ductile deformation and tectonic displacement was probably concentrated in the central serpentinite unit of the CSZ. During this event the serpentinite and the neighboring gneiss sheets were dismembered into slices a decameter to a hectometer thick and a hectometer to a kilometer long. The internal foliations of these megaboudins have consistent orientations as do the orientation of their boundaries with respect to the general trend of the principal thrust contact (Fig. 12b). The latter are either parallel or at an angle to the internal foliations and exhibit geometries akin to the *C* and *S* structures of mylonites. The shear sense deduced from the asymmetry of mesoscopic, anastomosed serpentinite foliations coincides with that deduced from map-scale patterns and microtectonic indicators of this and other units of the CSZ.

5.3. Section normal to the flow direction

Fig. 13a shows a reconstruction of the lateral equivalent of the CSZ and adjacent units relevant for the area of Fig. 3. Cartographic outlines of Fig. 3 were projected onto a plane perpendicular to L2 (trending N134°E and dipping 78° SW) whose orientation was determined from eigenvector calculation procedures as described above. Ductile flow is mainly perpendicular to the cross-section drawn, as highlighted with the stereoplots, also. In this reconstruction two main structural features must be discussed: the contacts between the Agudo Formation and the overlying Chimparra Gneiss, and the basal contacts of both, equivalent to the CSZ.

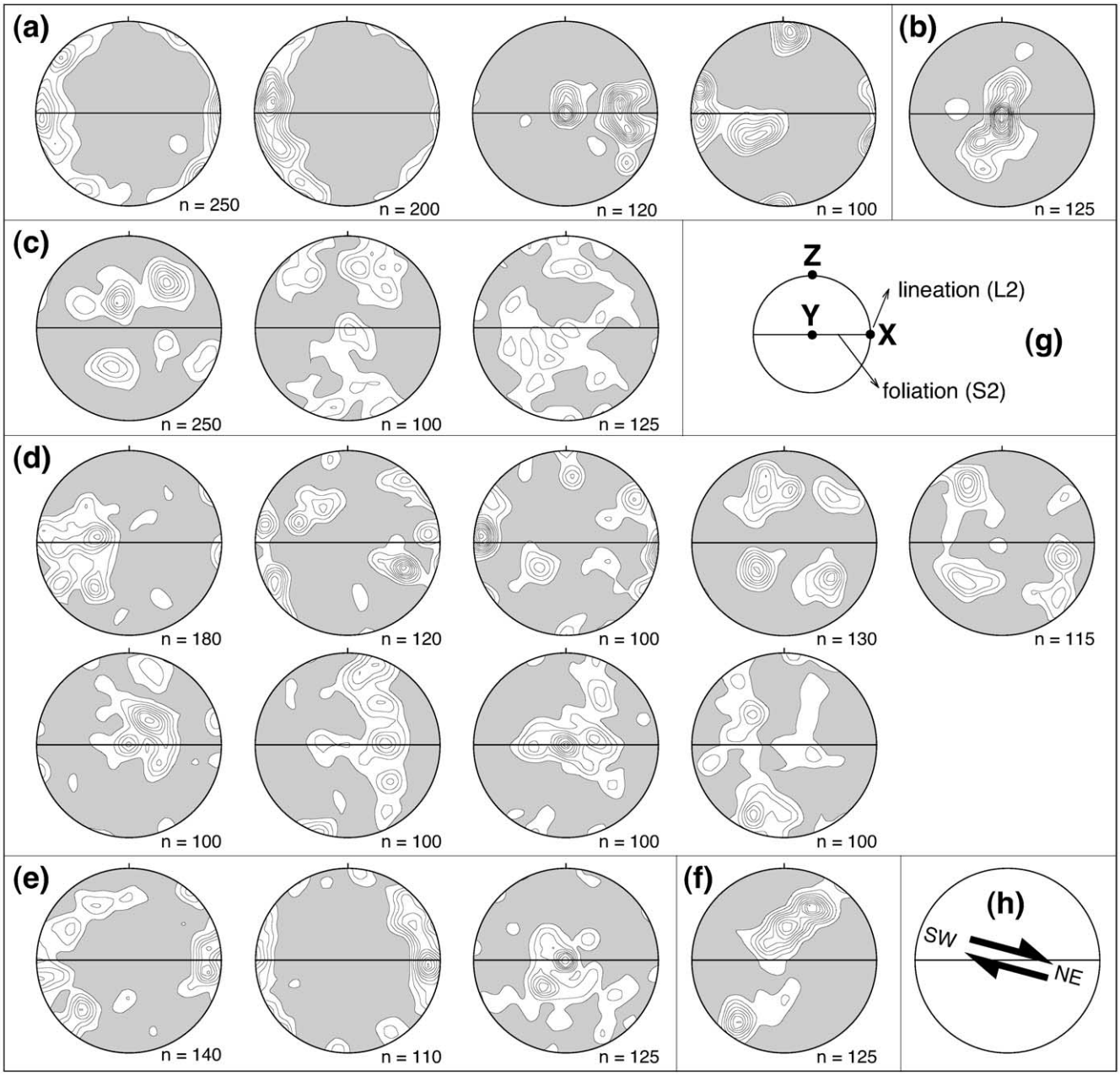

Fig. 8. Equal area, lower-hemisphere stereoplots (contours in multiples of uniform distribution) showing the *c*-axis fabrics measured in quartz veins parallel to the principal foliation (S2) of: (a) coarse-grained amphibolites of the Candelaria Formation, (b) fine-grained amphibolites of the Candelaria Formation, (c) gneisses (with high-pressure relics) of the eastern band of the CSZ, (d) gneisses of the western band of the CSZ, (e) amphibolites of the Purrido Formation, and (f) amphibolites of the Peña Escrita Formation. (g) Structural reference frame for the stereoplots. The projection plane of the stereoplots corresponds to a section perpendicular to the S2 foliation that contains the L2 lineation. (h) The sense of shear deduced from fabric asymmetry and microstructural observations in thin sections indicate a consistent top-to-the-NE movement of hanging wall blocks in spite of the variety of fabric patterns and intracrystalline slip systems involved.

The contact between the Agudo Formation and the Chimparra Gneiss is a thrust (delineated by serpentinite slivers) that puts higher-pressure rocks on top of slightly lower-pressure ones. This contact is folded into a complex surface (Figs. 3 and 10) in which various hinge zones can be recognized. These features have led in the past to interpret that a superposition of various folding episodes (isoclinal folds facing East and West, and open upright folds) had occurred (Engels, 1972; Bastida et al., 1984). In detail, two pairs of tight hinges and two pairs of gentler hinges can be identified. The former are connected in Fig. 13b with tie lines (that represent the traces of antiformal and synformal axial surfaces) subparallel to the basal thrust of the Upper Allochthon.

The long axes of elongated, eye-like closed features at the SE corner of Figs. 3 and 10 and depicted by foliation

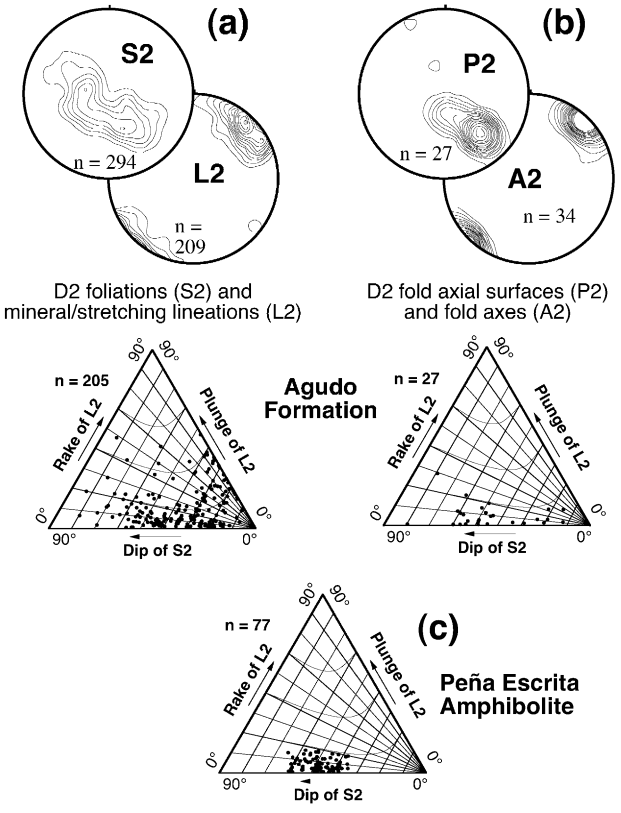

Fig. 9. (a) Equal area, lower-hemisphere stereoplots (contours in multiples of uniform distribution) and triangular diagrams showing the orientation of the principal foliation (S2) and lineation (L2), and of the pitch (rake) and plunge of L2 lineations and the dip of S2 foliations, respectively, in the Agudo Formation in the area shown in Fig. 3. (b) Idem as (a) for the orientation of the axial surface (P2) and the axes (A2) of coeval isoclinal folds, and for the pitch (rake) and plunge of A2 fold axes and the dip of P2 axial surfaces. (c) Triangular diagram showing the geometrical relationships between the principal foliation (S2) and lineation (L2) in the underlying Peña Escrita amphibolite in the area shown in Fig. 3.

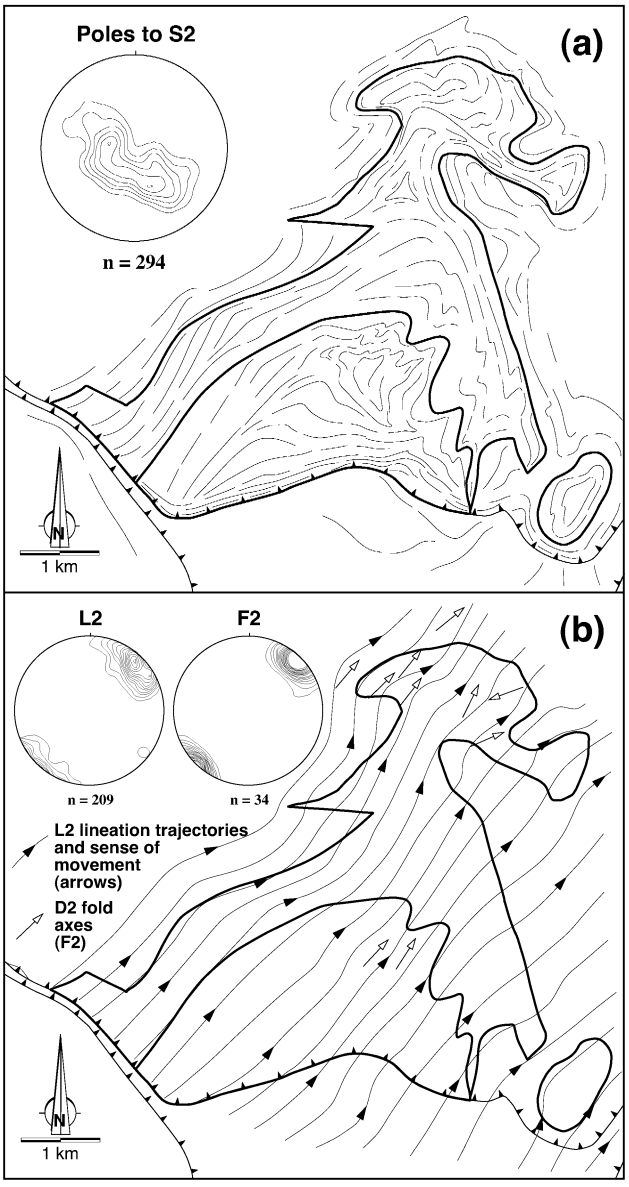

Fig. 10. (a) Structural map showing the trajectories of S2 foliations in the outcrop area of the Agudo Formation and adjacent units (see also Fig. 3). The stereoplot is a lower-hemisphere equal-area projection of the poles of S2 with contours in multiples of uniform distribution. (b) Structural map showing the trajectories of L2 lineations and the trend and plunge of D2 folds in the outcrop area of the Agudo Formation and adjacent units. The stereoplots are lower-hemisphere equal-area projections of the poles of L2 lineations and F2 fold axes, with contours in multiples of uniform distribution.

trajectories within the Agudo Formation (Figs. 10a and13b) are subparallel to the basal thrust of this unit and overlying gneisses onto their para-autochthon. Comparison of these features with the geometry of mesoscopic folds observed in *YZ* sections (e.g. Fig. 5d) enables us to interpret that the geometrical pattern of the upper contact of the Agudo Formation resulted from D2 sheath-like folding of a D1 thrust. In detail, this is a composite sheath formed by one first-order and various second-order folds. The amplitude of this composite sheath is ca. 1300 m and its width attains 6 km. The anvil-like folded surface of the structurally upper parts of the sheath and the isolated, closed outcrop to the East correspond to apical sections of second-order fold perturbations (Fig. 13b). The apical zone of the first order structure would lie within the outcrop on the less retrogressed metabasites with high-pressure relics. Note in Figs. 10a and 13b that in this unit S2 trajectories describe closed morphologies (the minor complexities there result from the influence of topographic highs and lows on gently dipping beds). In this scheme, retrogradation of the Agudo metabasites to amphibolites towards the upper contact with the Chimparra Gneiss would also be a tectonic feature related to deformation localization early during D2. Subsequent D2 deformation concentrated in the contact of both units with the underlying Peña Escrita Amphibolites.

The basal contact of the Agudo Formation and the Chimparra Gneiss cuts across the D1 thrust contact and the associated D2 lithostratigraphic variation described above. D2 foliations are subparallel to this contact along a

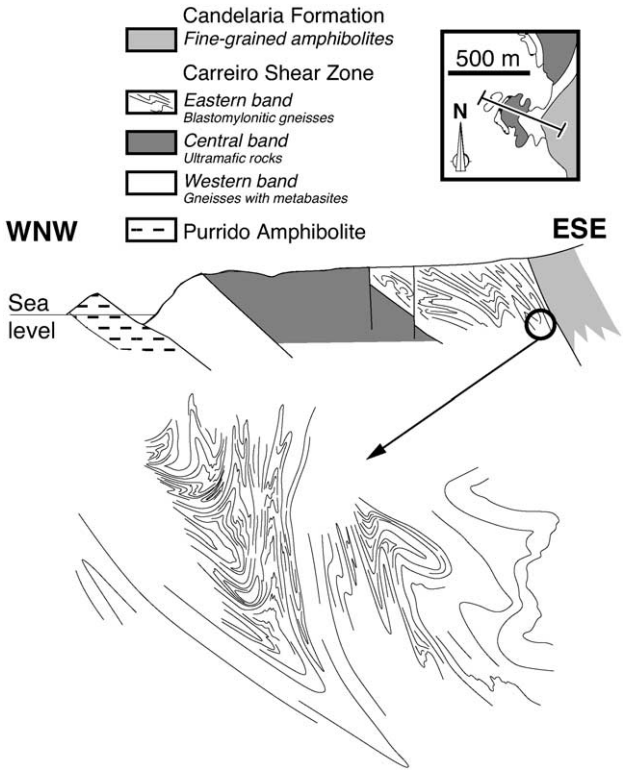

Fig. 11. Sketched geological map (see Fig. 2 for precise location) and cross-section of the Point Carreiro area showing: (i) the geometrical relationships between the principal units that crop out in the CSZ, and (ii) the intricate patterns of folding within specific units (after Bastida et al., 1984). Note the presence of refolded folds and closed eye-like structures, and that the plane of projection of these structures is normal to the regional trend of both folds and mineral stretching lineations, as presented in Figs. 5 and 6.

ca. 200–300-m-thick band in the hanging wall block except at the western end (Fig. 10a), where they are at a high angle. Various gabbro intrusions (up to 50 m thick and 500 m long) exist along this band, and exhibit lens-like geometries parallel to the basal thrust contact. From such geometrical relationships it can be interpreted that the intrusions postdated late D2 deformations. However, gabbro lenses exhibit a marked microstructural transition from coarse-grained meta-igneous textures (bearing coronitic garnet), through linear or planar–linear flaser gabbro, to laminated mylonitic amphibolite with fabrics like those (D2) described above. Consequently, gabbro intrusions record syn-tectonic D2 features and the basal shear zone of the Agudo Formation should be considered as a tectonic contact formed under relatively high temperature and pressure metamorphic conditions during D2.

The first order sheath and its lithostratigraphic variation are spatially related to a subarea of the Peña Escrita Amphibolites where a gradual transition occurs from a ca. 1000-m-thick metabasite pack to a 60-m-thick blanket that maintains its thickness along 6 km (until it joins the main outcrop of the Purrido Amphibolites in the western part of Cabo Ortegal). The reconstructed geometry of this transition (Fig. 13a) resembles a ramp. In detail, it consists of a flat to the West, a central ramp segment coincident with the core of the higher-grade Agudo rocks, and a second flat to the East (Fig. 13b). The dip angle of the ramp with respect to its flanking flats is of 25°, the change being accommodated gradually along ca. 500 m segments of increased curvature. This (lateral) ramp could have influenced the development of the major, kilometer-scale sheath fold, on one hand, and the position and orientation of the pair of NE-trending gentle structures that fold it, on the other hand. The latter folds (Fig. 13b) would be comparable with the trailing synforms and antiforms with foreland dipping axial surfaces formed in thrust hanging wall blocks at the flat–ramp and ramp–flat transitions of fault-bend folds in upper crustal settings (Boyer and Elliot, 1982). It is probable that both the hanging wall and footwall underwent deformation during thrusting, as the latter exhibits a synformal structure comparable with those described by Ramsay (1992).

6. Discussion and conclusions

Recognition and interpretation of the structures present in the Allochthonous Complexes of northwestern Iberia vary among different authors and among each klippe. After early theories on their origin, which related to an old Proterozoic basement or an early Paleozoic rift (Matte and Ribeiro, 1967; Vogel, 1967; Van Calsteren, 1977; Van Calsteren and Den Tex, 1978), the allochthonous model proposed by Ries and Shackleton (1971) and supported by Bayer and Matte's (1979) reinterpretation of previous geophysical data (Van Overmeeren, 1975; Keasberry, 1979) gained wide acceptance.

Currently, the debate concerns emplacement and exhumation kinematics of the complexes. A puzzling picture emerges when the ductile strain recorded by both the nappe units and their contacts is considered. Most thrust nappes, recumbent folds and detachments bear mineral and stretching lineations that are parallel to fold axes and trace the curvature of the Ibero–Armorican arc. In the nappe contacts (in fact, within the whole rock ensembles), stretching lineations with the same direction are parallel to the apical axes of sheath folds, whose meaning has thus been interpreted as marking the direction of tectonic transport (e.g. Iglesias et al., 1983). These directions can vary in the different allochthonous complexes: N160E-trending and SSE-verging in Bragança and Morais (Anthonioz, 1972; Marques et al., 1992), N100-120E-trending and E-verging (Díaz García et al., 1999a,b) in Órdenes, and N000-040E-trending and NNE-verging in eastern (Martínez Catalán and Arenas, 1992) and western (Van Zuuren, 1969) parts of Órdenes, Cabo Ortegal (Girardeau and Gil Ibarguchi, 1991; Ábalos et al., 1994; Marcos and Farias, 1999), and Malpica–Tuy (Gil Ibarguchi and Ortega Gironés, 1985). Fernández (1993) and Llana Fúnez (1999) recognized NNE lineations in blastomylonitic foliations in Cabo

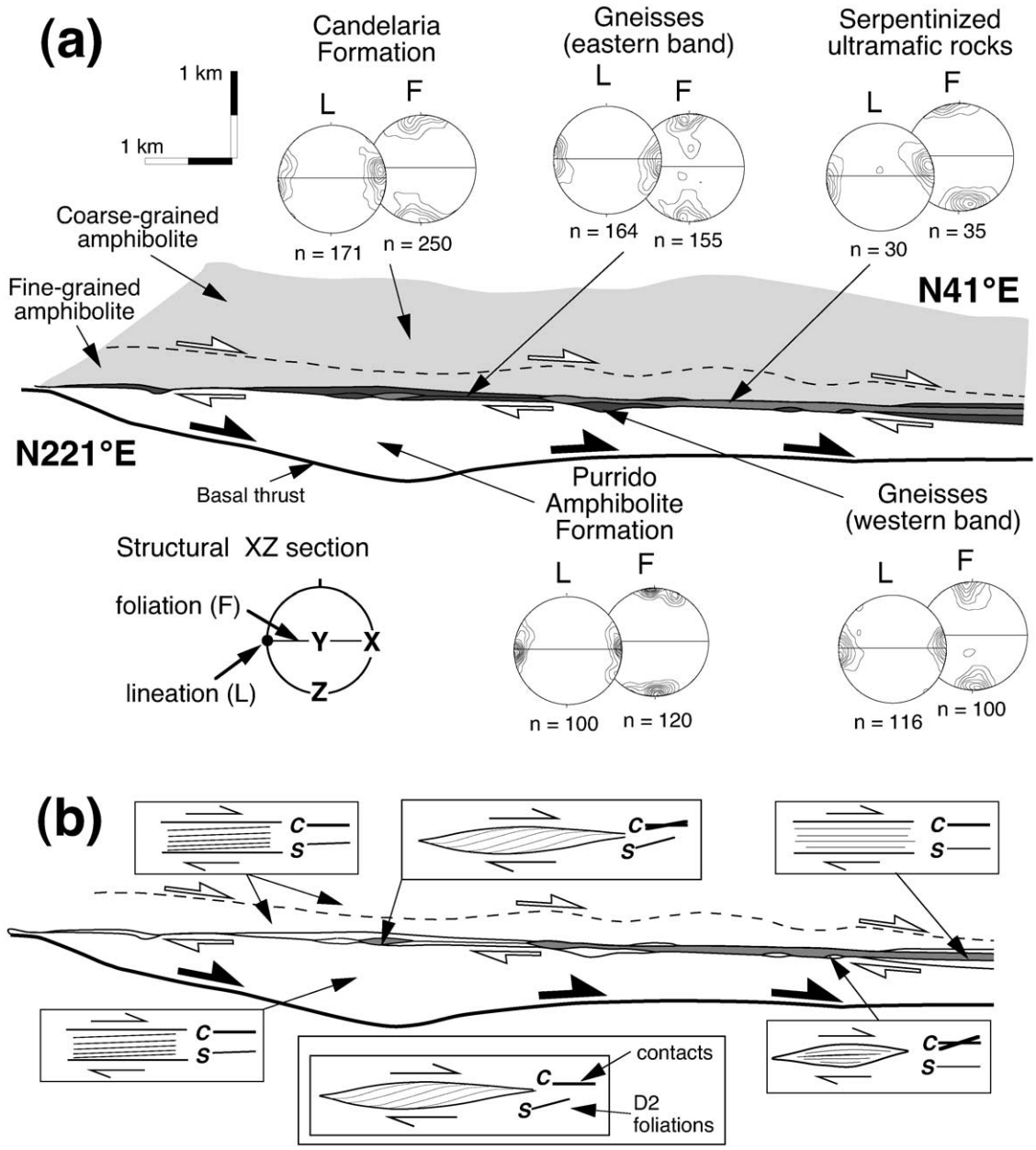

Fig. 12. (a) Structural reconstruction (in a projection perpendicular to regional foliation that contains the lineation) of the likely geometry of the CSZ and the adjacent units. The strike of the projection plane is N041°E and the dip is 50° NW. In the lower-hemisphere equal-area plots (with contours in multiples of uniform distribution), S2 foliations and L2 lineations presented in Fig. 5 have been rotated so that the equatorial section is parallel to the projection plane of the cross-section. In this new structural framework foliations and lineations plot as point maxima centered on the *Z* and *X* directions, respectively, showing the relative geometrical orientation of flow planes (*XY*/S2) and flow directions (*X*/L2). (b) Sketch of the reconstructed section shown in (a) depicting the geometrical relationships between the tectonic boundaries ('C' contacts) of serpentinite and gneiss slices and the attitude of D2 foliations ('S' planes) within them. The resultant patterns are similar to different types of *S–C* structures that associate top-to-the-NE sense of movement of hanging wall blocks.

Ortegal and Malpica–Tuy, respectively, but they did not relate them to either NNE- or SSW-directed kinematics.

Often, it is assumed after Bastida et al. (1984) and Marcos et al. (1984) that the transport direction of nappes was basically toward the foreland (situated to the East). All this is based upon the fact that the trends of earlier Variscan structures describe the curvature of the Ibero–Armorican arc, and upon the apparent vergence of fold structures and the presumed direction of propagation of thrusts toward the arc center. This constituted also a valuable effort to correlate the tectonic evolution of the Allochthonous Complexes with that of other major tectonostratigraphic units or terranes across the orogen by means of a small number of deformation and metamorphism phases (e.g. Pérez Estaún et al., 1991). The way in which cross-sections of the Allochthonous Complexes have been described so far has been influenced to a great extent by that perspective, notably as regards the vergence of large isoclinal folds, their

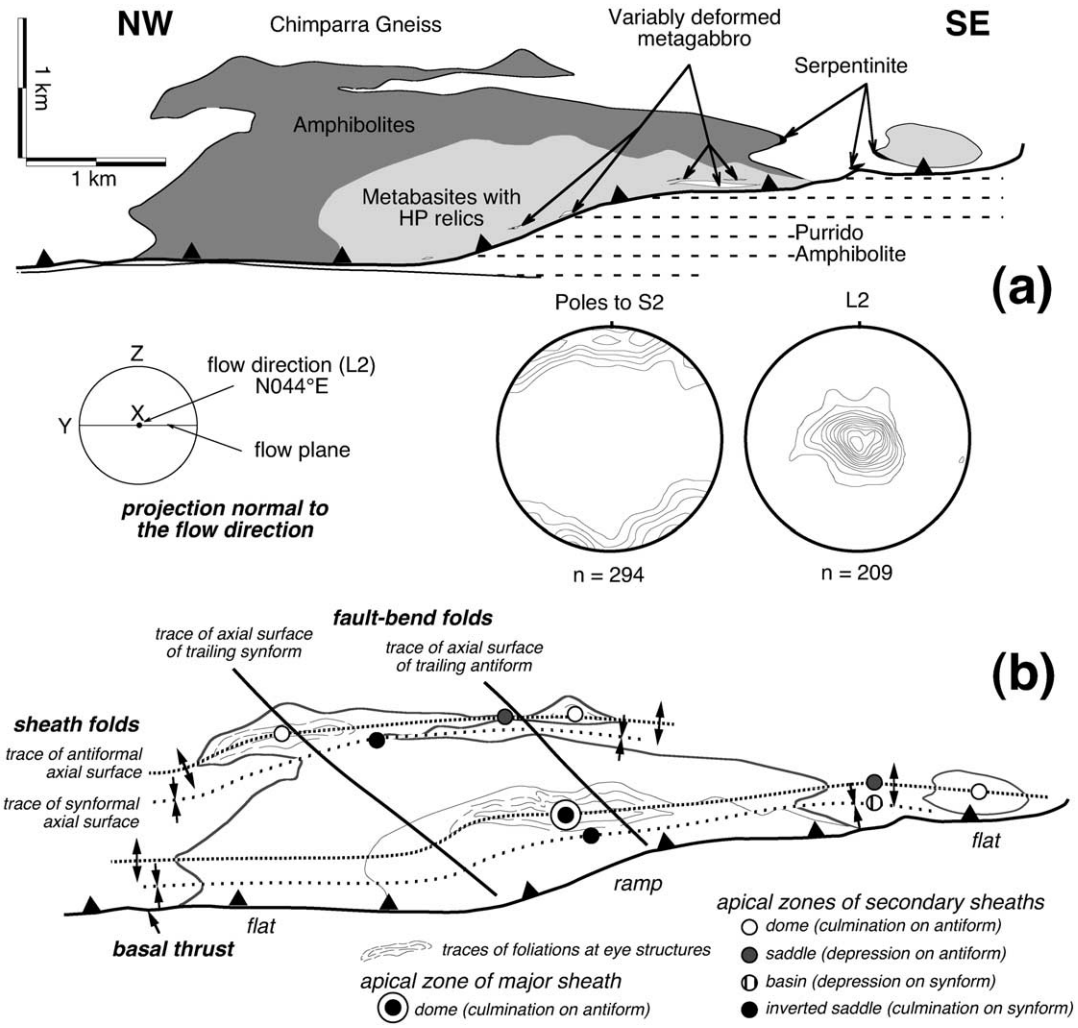

Fig. 13. (a) Structural reconstruction of a down-plunge projection (perpendicular to the regional lineation L2) of the likely geometry of the outcrop area of the Agudo Formation (see also Fig. 3). The strike of the projection plane is N134°E and the dip is 78° SW. In the lower-hemisphere equal-area plots (with contours in multiples of uniform distribution), S2 foliations and L2 lineations presented in Fig. 9 have been rotated so that the equatorial section is parallel to the projection plane of the cross-section. In this new structural framework foliations and lineations plot as point maxima centered on the *Z* and *X* directions, respectively, showing the relative geometrical orientation of flow planes (*XY*/S2) and flow directions (*X*/L2). (b) Sketched drawing of (a) showing the structural interpretation of fold-related structures. The nomenclature of sheath fold apical axes and axial surfaces follows the scheme proposed by Alsop and Holdsworth (1999). See text for further details.

geometrical evolution at depth (e.g. Fig. 14a), the occurrence of major thrusts (or the lack of them), and even the order of superposition of units making more or less complete postulated coherent sections of the lower crust and the uppermost mantle (e.g. Galán and Marcos, 1997, 2000).

The general deformational scheme proposed originally by Bastida et al. (1984) and Marcos et al. (1984) for the Cabo Ortegal complex was based upon geometrical superposition criteria and minor fold interference patterns. After the high-grade metamorphic episodes, a first deformation phase (D1) gave rise to a mylonitic foliation. D1 foliations were folded during a second deformation phase (D2) by large, asymmetric, ca. N–S trending and East-verging isoclinal folds. In general, neither major nor minor D2 folds produced new axial planar foliations. D2 folds were cut by thrusts during D3, which gave rise to development of new folds (homoaxial with D2 folds) and discrete shear zones facing East, also. Descriptions of D3 structures included sheath folds whose axial dispersion was pointed out as the cause of erroneous attribution of folds to episodes of deformation by previous authors. D4 gave rise to open upright folds homoaxial with the previous ones. As regards the kinematic interpretation of the regional NNE-trending lineations following the conventional criteria, Fernández (1993) and Marcos (1998) argued that it is not reliable based upon the following criteria: (i) most lineations are interpreted as intersection lineations between the mylonitic foliation and a previous banding; (ii) mineral lineations, when they occur, are defined by the elongation of late, retrograde minerals, and thus do not relate to the higher-grade metamorphic events; (iii) the observed kinematic indicators can be equivocal

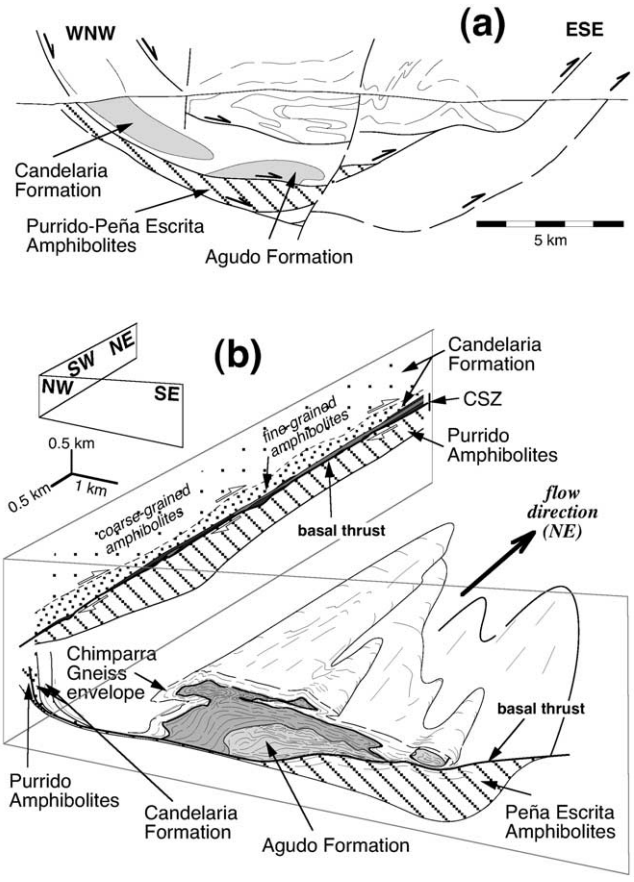

Fig. 14. (a) Conventional interpretation of the structure and kinematics of the Cabo Ortegal nappe after Bastida et al. (1984) and Marcos et al. (1984). The WNW–ESE cross-section (sketched for simplicity) and the top-to-the-ESE tectonic displacements are barely perpendicular to the regional structural trends.(b) Three-dimensional reconstruction of the geometry and kinematics of the lower nappes of the Cabo Ortegal high-grade and high-pressure allochthon as proposed in this paper. Intense non-coaxial deformations in a context of top-to-the-NE ductile flow gave rise to imbrication and kilometer-scale sheath fold development in the CSZ and the equivalent structural domains, respectively.

even within single outcrops; and (iv) fold superposition would have entangled the kinematic pattern.

Our tectonic interpretations differ from that described above in: (i) the number of deformation phases, (ii) their meaning and adscription from a metamorphic perspective, (iii) the type and geometry of the structures recognized, and (iv) their kinematic significance. In Fig. 14b a three-dimensional reconstruction of D2 structures based upon two panels (trending NE–SW and NW–SE) shows the geometry of the thrust zone involving the lower nappes of the Upper Allochthon and the upper nappes of the underlying Ophiolitic Unit. Nappe units are akin to type-F, fold related, lobe-shaped crystalline thrust sheets of Hatcher and Hooper (1992). These may form in A- or B-subduction settings below the ductile–brittle transition and their penetrative fabrics record transport and deformation of the entire sheets. The dimensions of the units are larger in the direction of the ductile flow and much shorter across. First- and second-order kilometer-scale sheath folds formed in Cabo Ortegal due to lithological heterogeneity associated with D2 syntectonic retrogression and with contortion of ductile thrust surfaces. Their apical axes are parallel to the NE direction of rock flow also deduced from microstructural analysis. This and the contractional deformation components described in the plane normal to that direction are congruent with finite strain ellipsoids after progressive D2 bearing: (i) long axes (X) parallel to the NE direction and accommodating true stretching, (ii) SE-trending intermediate axes (Y) accommodating true shortening, and (iii) subvertical short axes (Z) accommodating still larger shortening components. These are ellipsoids of general constriction and formed under non-coaxial deformation increments.

The primary orientation of the basal thrust of the Upper Allochthon is presented in Fig. 14b as a subhorizontal rugged surface. However, it was probably a dipping surface when active during Hercynian subduction and collision. Depending on the strike and dip of the movement zone relative to the orientation of the flow direction, various situations can arise ranging between dip-slip and strike-slip. If the subduction zone were subparallel to the trend of the actual orogen, in NW Iberia it would trend near N–S. As regards the polarity of subduction (dip sense), whilst some authors have proposed an E-dipping plane (e.g. Iglesias et al., 1983; Dias and Ribeiro, 1995) most authors favor a W-dipping one (Bard et al., 1980; Matte, 1986, 1991; Burg et al., 1987; Arenas et al., 1997; Martínez Catalán et al., 1997). These authors assume in preference orogen-normal tectonic displacements, which are implied in their lithospheric-scale cross-sections. However, since orientation of flow directions is subparallel to the strike of crustal subduction planes, these ought to be interpreted in terms of orogen-parallel tectonic displacements due to oblique plate convergence. Only a few authors have followed explicitly this line of thinking. Badham (1982), Vauchez and Nicolas (1991) and Shelley and Bossière (2000) point to large dextral tectonic displacements along the suture of the Hercynian orogen. Martínez Catalán (1990), by contrast, suggested that the allochthonous complexes of NW Iberia were emplaced from North to South, thus implying sinistral displacements along the suture.

In order to reconcile these apparently incompatible views, we argue that orogen-normal tectonic displacements represent minor components of the relative displacement between the intervening plates during Hercynian orogeny. Though the former could have attained a few hundreds of kilometers, the principal displacement was sub-parallel to the orogen and probably one order of magnitude larger (i.e. a few thousands of kilometers). This interpretation reconciles the geometry of conventional cross-sections published so far and the kinematics of deformation deduced from pervasive foliations containing orogen-parallel, mineral and stretching lineations. Llana Fúnez (1999) makes reference to alternative kinematic models such as the rolling of dough (Lister and Price, 1978), which implies that

predominant simple shear components are normal to the lineation. Such situations are known in transpression zones and record characteristic microstructures (Jiang and White, 1995; Jiang et al., 2001). However, microstructural evidence described so far in the areas discussed here does not support such a model.

The structures described in this paper are rare examples of thrust nappes formed in lower crustal settings where it is difficult to apply many of the analytical techniques used when dealing with upper crustal thrust structures. Those nappes put higher-pressure rocks onto lower-pressure ones and the units involved record some deformation-related retrogression. This might suggest that emplacement and exhumation of high-pressure nappes were coeval in Cabo Ortegal. In the neighboring Órdenes complex some major detachments have been mapped that postdate ductile thrusts and put lower pressure rocks onto higher pressure ones (e.g. Martínez Catalán et al., 1996, 1997; Díaz García et al., 1999a). These detachments are thought to have controlled the exhumation of deep crustal units of the Allochthonous Complexes in general and are often characterized by extension components parallel to the orogenic trends. In Cabo Ortegal, such structures are absent, but there exist discrete, extensional (D3) low-angle shears (Ábalos et al., 1994) that postdate the thrusts nappe structures and their internal fabrics described in this paper. This can be due to the fact that in Cabo Ortegal only the basal, higher-pressure units of the regional Upper Allochthon (Fig. 1a) crop out, and the exotic (lower-pressure) hanging wall has been removed by erosion.

Acknowledgements

We are grateful to David Shelley and Gabriel Gutiérrez Alonso, whose reviews helped to improve the quality of the paper. This study was financially supported by the Spanish DGICYT (grants PB97-617 and PB98-0143).

References

Ábalos, B., 1997. Omphacite fabric variation in the Cabo Ortegal eclogite (NW Spain): relationships with strain symmetry during high-pressure deformation. Journal of Structural Geology 19, 621–637.

Ábalos, B., Mendia, M.S., Gil Ibarguchi, J.I., 1994. Structure of the Cabo Ortegal eclogite-facies zone (NW Iberia). Comptes Rendus de l'Académie des Sciences de Paris 319, 1231–1238.

Ábalos, B., Azcárraga, J., Gil Ibarguchi, J.I., Mendia, M.S., Santos Zalduegui, J.F., 1996. Flow stress, strain rate and effective viscosity evaluation in a high-pressure nappe (Cabo Ortegal, Spain). Journal of Metamorphic Geology 14, 227–248.

Ábalos, B., Azcárraga, J., Gil Ibarguchi, J.I., Mendia, M.S., Puelles, P., 2000. Mapa Geológico del Complejo de Cabo Ortegal (NO de España). Instituto Universitario de Xeoloxía Isidro Parga Pondal, scale 1:42.750.

Alsop, G.I., Holdsworth, R.E., 1999. Vergence and facing patterns in large-scale sheath folds. Journal of Structural Geology 21, 1335–1349.

Anthonioz, P.M., 1972. Les complexes polymétamorphiques précambriens de Morais et Bragança (NE du Portugal): étude pétrographique et structurale. Memórias dos Serviços Geológicos de Portugal 20, 1–112.

Arenas, R., 1991. Opposite *P–T–t* paths of Hercynian metamorphism between the upper units of the Cabo Ortegal Complex and their substratum (northwest of Iberian Massif). Tectonophysics 191, 347–364.

Arenas, R., Abati, J., Martínez Catalán, J.R., Díaz García, F., Rubio Pascual, F.J., 1997. *P–T* evolution of eclogites from the Agualada Unit (Ordenes Complex, northwest Iberian Massif, Spain): implications for crustal subduction. Lithos 40, 221–242.

Arps, C.E.S., Van Calsteren, P.W.C., Hilgen, J.D., Kuijper, R.P., Den Tex, E., 1977. Mafic and related complexes in Galicia: an excursion guide. Leidse Geologische Mededelingen 51, 63–94.

Azcárraga, J., 1998. Evolución tectónica y metamórfica de los mantos inferiores de grado alto y alta presión del complejo de Cabo Ortegal. Ph.D. thesis, Universidad del País Vasco.

Badham, J.P.V., 1982. Strike-slip orogens; an explanation for the Hercynides. Journal of the Geological Society of London 139, 493–504.

Bard, J.P., Burg, J.P., Matte, Ph., Ribeiro, A., 1980. La Chaîne Hercynienne d'Europe occidentale en termes de Tectonique des Plaques. In: Géologie de l'Europe, du Précambrien aux basins sédimentaires post-Hercyniennes. Mémoires du Bureau de Recherches Géologiques et Minières 108, pp. 233–246.

Basterra, R., Cassi, J.M., Pérez de San Román, L., Tascón, A., Gil Ibarguchi, J.I., 1988. Evolución metamórfica de las rocas pelíticas y semipelíticas de las formaciones "Banded Gneisses" y "Gneises de Cariño" (Cabo Ortegal, NO España). Studia Geologica Salmanticensia, volumen especial 4, 131–144.

Bastida, F., Marcos, A., Marquínez, J., Martínez Catalán, J.R., Pérez Estaún, A., Pulgar, J.A., 1984. Mapa Geológico de España, Hoja no. 1, La Coruña. Instituto Geológico y Minero de España, scale 1:200.000.

Baudin, T., Marquer, D., Persoz, F., 1993. Basement-cover relationships in the Tambo nappe (Central Alps, Switzerland): geometry, structure and kinematics. Journal of Structural Geology 15, 543–553.

Bayer, R., Matte, Ph., 1979. Is the mafic/ultramafic massif of Cabo Ortegal (northern Spain) a nappe emplaced during a Variscan obduction?—A new gravity interpretation. Tectonophysics 57, T9–T18.

Boyer, S., Elliot, D., 1982. Thrust systems. American Association of Petroleum Geologists Bulletin 66, 1196–1230.

Burg, J.P., Balé, P., Brun, J.P., Girardeau, J., 1987. Stretching lineations and transport direction in the Ibero–Armorican Arc during the Siluro–Devonian collision. Geodinamica Acta 1, 71–81.

Carreras, J., 2001. Zooming on Northern Cap de Creus shear zones. Journal of Structural Geology 23, 1457–1486.

Dallmeyer, R.D., Gil Ibarguchi, J.I., 1990. Age of the amphibolitic metamorphism in the Ophiolitic Unit of the Morais allochthon (Portugal): implications for early Hercynian orogenesis in the Iberian massif. Journal of the Geological Society of London 147, 873–878.

Dallmeyer, R.D., Ribeiro, A., Marques, F., 1991. Polyphase Variscan emplacement of exotic terranes (Morais and Bragança Massifs) onto Iberian successions: evidence from $^{40}Ar/^{39}Ar$ mineral ages. Lithos 27, 133–144.

Dallmeyer, R.D., Martínez Catalán, J.R., Arenas, R., Gil Ibarguchi, J.I., Gutiérrez Alonso, G., Farias, P., Bastida, F., Aller, J., 1997. Diachronous variscan tectonothermal activity in the NW Iberian Massif: evidence from $^{40}Ar/^{39}Ar$ dating of regional fabrics. Tectonophysics 277, 307–337.

De Paor, D.G., 1988. Rf/ϕ strain analysis using an orientation net. Journal of Structural Geology 10, 823–833.

Den Tex, E., 1981. A geological section across the Hesperian Massif in western and central Galicia. Geologie in Mijnbouw 60, 33–40.

Dias, R., Ribeiro, A., 1995. The Ibero–Armorican arc: a collision effect against an irregular continent? Tectonophysics 246, 113–128.

Díaz García, F., Martínez Catalán, J.R., Arenas, R., González Cuadra, P., 1999a. Structural and kinematic analysis of the Corredoiras detachment: evidence for early Variscan syn-convergent extension. International Journal of Earth Sciences 88, 337–351.

Díaz García, F., Arenas, R., Martínez Catalán, J.R., González del Tánago, J., Dunning, G., 1999b. Tectonic evolution of the Careón ophiolite

(Northwest Spain): a remnant of oceanic lithosphere in the Variscan belt. Journal of Geology 107, 587–605.

Engels, J.P., 1972. The catazonal poly-metamorphic rocks of Cabo Ortegal (NW Spain), a structural and petrographic study. Leidse Geologische Mededelingen 48, 83–133.

Engels, J.P., Hubregtse, J.J.M.W., Floor, P., Den Tex, E., 1974. Precambrian complexes in the Hercynian orogen of the Northwestern Iberian Peninsula. In: Precambrien des zones mobiles de l'Europe, Conference de Liblice (1972), pp. 163–173.

Fernández, F.J., 1993. La deformación de los gneises de Chimparra en Punta Tarroiba (Cabo Ortegal, NW de España). Revista de la Sociedad Geológica de España 6, 77–91.

Fernández, F.J., 1994. Estructuras desarrolladas en gneises bajo condiciones de alta P y T (gneises de Chímparra, Cabo Ortegal, A Coruña, Galicia, España). Ph.D. thesis, Universidad de Oviedo.

Galán, G., Marcos, A., 1997. Geochemical evolution of the high-pressure mafic granulites from the Bacariza formation (Cabo Ortegal complex, NW Spain): an example of a heterogeneous lower crust. Geologische Rundschau 86, 539–555.

Galán, G., Marcos, A., 2000. The metamorphic evolution of the high-pressure mafic granulites of the Bacariza Formation (Cabo Ortegal Complex, Hercynian belt, NW Spain). Lithos 54, 139–171.

Gil Ibarguchi, J.I., Ortega Gironés, E., 1985. Petrology, structure and geotectonic implications of glaucophane-bearing eclogites and related rocks from Malpica–Tuy (MT) Unit, Galicia, Northwest Spain. Chemical Geology 50, 145–162.

Gil Ibarguchi, J.I., Ábalos, B., Campillo, A., Higuero, A., López, B., Pinilla, V., Rodríguez, C., Rodríguez, R., Urtiaga, K., 1987. Asociaciones con granate-clinopiroxeno en la unidad catazonal superior del complejo de Cabo Ortegal. Cuadernos del Laboratorio Xeolóxico de Laxe 12, 165–181.

Gil Ibarguchi, J.I., Mendia, M., Girardeau, J., Peucat, J.J., 1990. Petrology of eclogites and clinopyroxene–garnet metabasites from the Cabo Ortegal Complex (northwestern Spain). Lithos 25, 133–162.

Gil Ibarguchi, J.I., Ábalos, B., Azcárraga, J., Puelles, P., 1999. Deformation, high-pressure metamorphism and exhumation of ultramafites in a deep subduction/collision setting (Cabo Ortegal, NW Spain). Journal of Metamorphic Geology 17, 747–764.

Girardeau, J., Gil Ibarguchi, J.I., 1991. Pyroxenite-rich peridotites of the Cabo Ortegal Complex (Northwestern Spain): evidence for large-scale upper-mantle heterogeneity. Journal of Petrology, Special Lherzolites Issue, pp. 135–154.

Goscombe, B., 1991. Intense non-coaxial shear and the development of mega-scale sheath folds in the Arunta Block. Central Australia. Journal of Structural Geology 13, 299–318.

Hatcher, R.D., Hooper, R.J., 1992. Evolution of crystalline thrust sheets in the internal parts of mountain belts. In: McClay, K.R. (Ed.). Thrust Tectonics. Chapman & Hall, London, pp. 217–233.

Hibbard, J., Karig, D.E., 1987. Sheath-like folds and progressive fold deformation in Tertiary sedimentary rocks of the Shimanto accretionary complex, Japan. Journal of Structural Geology 9, 845–857.

Hillner, U., 1995. I. Die Geologie der Basalen Ophiolith-Einheit am Westrand des Cabo Ortegal Komplexes in Galizien, NW-Spanien. II. Kontrastierende Druck-Temperatur-Entwicklungen basaler Kristallindecken am Westrand des Cabo Ortegal Komplexes in Galizien, NW-Spanien. Unveröffentlichte Diplomarbeit, Christian Albrechts Universität, Kiel.

Iglesias, M., Ribeiro, M.L., Ribeiro, A., 1983. La interpretación aloctonista de la estructura del Noroeste Peninsular. In: Libro Jubilar J.M. Ríos—Geología de España, vol. 1. Publicaciones del Instituto Geológico y Minero de España, pp. 459–467.

Jiang, D., White, J.C., 1995. Kinematics of rock flow and the interpretation of geological structures, with particular reference to shear zones. Journal of Structural Geology 17, 1249–1265.

Jiang, D., Lin, S., Williams, P.F., 2001. Deformation paths in high-strain zones, with reference to slip partitioning in transpressional plate-boundary regions. Journal of Structural Geology 23, 991–1005.

Keasberry, E., 1979. An interpretation model of semi-circular Bouguer anomalies found over the peripheral belt of the Ordenes Complex (NW Spain). Geologie en Mijnbouw 58, 65–70.

Kelly, N.M., Clarke, G.L., Carson, C.J., White, R.W., 2000. Thrusting in the lower crust: evidence from the Oygarden Islands, Kemp Land, East Antarctica. Geological Magazine 137, 219–234.

King, J.E., 1986. The metamorphic internal zone of Wopmay Orogen (Early Proterozoic), Canada: 30 km of structural relief in a composite section based on plunge projection. Tectonics 5, 973–994.

Kleinschrodt, R., Vollmer, G., 1994. Deformation and metamorphic evolution of a large-scale fold in the lower crust: the Dumbara synform, Sri Lanka. Journal of Structural Geology 16, 1495–1507.

Kuijper, R.P., Priem, H.N.A., Den Tex, E., 1982. Late Archean–Early Proterozoic source ages of zircons in rocks from the Paleozoic Orogen of Western Galicia, NW Spain. Precambrian Research 19, 1–29.

Lister, G.S., Price, G.P., 1978. Fabric development in a quartz–feldspar mylonite. Tectonophysics 49, 37–78.

Llana Fúnez, S., 1999. La estructura de la Unidad e Malpica–Tui (Cordillera Varisca en Iberia). Ph.D. thesis, Universidad de Oviedo.

Mainprice, D., Bouchez, J.L., Blumenfeld, Ph., Tubía, J.M., 1986. Dominant -c- slip in naturally deformed quartz: implications for dramatic softening at high temperature. Geology 14, 819–822.

Mancktelow, N.S., 1990. STEREOPLOT. Computer Program + Users Guide and Reference Manual.

Marcos, A., 1998. La estructura del Complejo de Cabo Ortegal (NW de España). Geologos 2, 15–22.

Marcos, A., Farias, P., 1999. La estructura de las láminas inferiores del Complejo de Cabo Ortegal y su alóctono relativo (Galicia, NO de España). Trabajos de Geología 21, 201–218.

Marcos, A., Marquínez, J., Pérez-Estaún, A., Pulgar, J.A., Bastida, F., 1984. Nuevas aportaciones al conocimiento de la evolución tectono-metamórfica del Complejo de Cabo Ortegal. Cuadernos del Laboratorio Xeoloxico de Laxe 7, 125–137.

Marques, F.G., Ribeiro, A., Pereira, E., 1992. Tectonic evolution of the deep crust: Variscan reactivation by extension and thrusting of Precambrian basement in the Bragança and Morais Massifs (Trás-os-Montes, NE Portugal). Geodinamica Acta 5, 135–151.

Martínez Catalán, J.R., 1990. A non-cylindrical model for the northwest Iberian allochthonous terranes and their equivalents in the Hercynian belt of Western Europe. Tectonophysics 179, 253–272.

Martínez Catalán, J.R., Arenas, R., 1992. Deformación extensional de las unidades alóctonas superiores de la parte oriental del Complejo de Órdenes (Galicia). Geogaceta 11, 108–111.

Martínez Catalán, J.R., Arenas, R., Díaz García, F., Rubio Pascual, F.J., Abati, J., Marquínez, J., 1996. Variscan exhumation of a subducted paleozoic continental margin: the basal units of the Ordenes Complex, Galicia, NW Spain. Tectonics 15, 106–121.

Martínez Catalán, J.R., Arenas, R., Díaz García, F., Abati, J., 1997. Variscan accretionary complex of northwest Iberia: terrane correlation and succession of tectonothermal events. Geology 25, 1103–1106.

Mattauer, M., Collot, B., Van Den Driessche, J., 1983. Alpine model for the internal metamorphic zones of the North American Cordillera. Geology 11, 11–15.

Matte, Ph., 1986. Tectonics and plate tectonics model for the Variscan Belt of Europe. Tectonophysics 126, 329–374.

Matte, Ph., 1991. Accretionary history and crustal evolution of the Variscan belt in Western Europe. Tectonophysics 196, 309–337.

Matte, P., Ribeiro, A., 1967. Les rapports tectoniques entre le Précambrienn ancien et le Paléozoïque dans le Nord-Ouest de la Péninsule Ibérique: grandes nappes ou extrusions? Comptes Rendus de l'Académie des Sciences de Paris 264, 2268–2271.

Ordóñez, B., Gebauer, D., Schäfer, H.-J., Gil Ibarguchi, J.I., Peucat, J.J., 2001. A single Devonian subduction event for the HP/HT metamorphism of the Cabo Ortegal Complex within the Iberian Massif. Tectonophysics 232, 359–385.

Passchier, C.W., 1987. Stable positions of rigid objects in non-coaxial

flow—a study in vorticity analysis. Journal of Structural Geology 9, 679–690.

Passchier, C.W., 1994. Mixing in flow perturbations: a model for development of mantled porphyroclasts in mylonites. Journal of Structural Geology 16, 733–736.

Passchier, C.W., Trouw, R.A.J., 1996. Microtectonics. Springer, Berlin, Heidelberg.

Pérez Estaún, A., Martínez Catalán, J.R., Bastida, F., 1991. Crustal thickening and deformation sequence in the footwall to the suture of the Variscan belt of northwest Spain. Tectonophysics 191, 243–253.

Peucat, J.J., Bernard-Griffiths, J., Gil Ibarguchi, J.I., Dallmeyer, R.D., Menot, R.P., Cornichet, J., Iglesias Ponce de León, M., 1990. Geochemical and geochronological cross section of the deep Variscan crust: the Cabo Ortegal high-pressure nappe (NW Spain). Tectonophysics 177, 263–292.

Pin, C., Paquette, J.L., Gil Ibarguchi, J.I., Santos Zalduegui, J.F., Rodríguez Aller, J., Ortega Cuesta, L.A., 2000. Geochronological and geochemical constraints on the origin of ophiolitic units from the northwestern Iberian Massif. Basement Tectonics 15, Abstract, La Coruña.

Ramsay, J.G., 1967. Folding and Fracturing of Rocks. McGraw-Hill, New York.

Ramsay, J.G., 1992. Some geometric problems of ramp-flat thrust models. In: McClay, K.R. (Ed.). Thrust Tectonics. Chapman & Hall, London, pp. 191–200.

Ries, A., Shackleton, R.M., 1971. Catazonal complexes of north-western Spain and north Portugal; remnants of a Hercynian thrust plate. Natural and Physical Science 234, 65–69.

Sander, B., 1930. Gefügekunde der Gesteine. Springer, Berlin, Vienna.

Santos Zalduegui, J.F., Schärer, U., Gil Ibarguchi, J.I., 1996. Isotope constraints on the age and origin of magmatism and metamorphism in the Malpica–Tuy Allochthon. Chemical Geology 121, 91–103.

Santos Zalduegui, J.F., Schärer, U., Gil Ibarguchi, J.I., Girardeau, J.J., 1997. Origin and evolution of the Paleozoic Cabo Ortegal ultramafic–mafic complex (NW Spain): U–Pb, Rb–Sr and Pb–Pb isotope data. Chemical Geology 129, 281–304.

Santos Zalduegui, J.F., Schärer, U., Gil Ibarguchi, J.I., Girardeau, J., 2002. Genesis of pyroxenite-rich peridotite at Cabo Ortegal (NW Spain): geochemical and Pb–Sr–Nd isotope data. Journal of Petrology 43, 17–43.

Shackleton, R., 1993. Tectonics of the lower crust: a view from the Usambara Mountains, NE Tanzania. Journal of Structural Geology 15, 663–671.

Shelley, D., Bossière, G., 2000. A new model for the Hercynian Orogen of Gondwanan France and Iberia. Journal of Structural Geology 22, 757–776.

Simpson, C., 1992. Kinematic analysis in general shear mylonite zones. III Congreso Geológico de España y VIII Congreso Latinoamericano de Geología, vol. 2, pp. 431–438.

Simpson, C., De Paor, D.G., 1993. Strain and kinematic analysis in general shear zones. Journal of Structural Geology 15, 1–20.

Truesdell, C., 1954. The Kinematics of Vorticity. Indiana University Press, Bloomington.

Van Calsteren, P.W.C., 1977. Geochronological, geochemical and geophysical investigations in the Hercynian basement of Galicia (NW Spain). Leidse Geologische Mededelingen 51, 57–61.

Van Calsteren, P.W.C., Den Tex, E., 1978. An early Paleozoic continental rift system in Galicia (NW Spain). In: Ramberg, J.B., Neuman, E.R. (Eds.). Tectonics and Geophysics of Continental Rifts. Reidel, Dordrecht, pp. 125–132.

Van Calsteren, P.W.C., Boelrijk, N.A.I.M., Hebeda, E.H., Priem, H.N.A., Den Tex, E., Verdurmen, E.A.T., Verschure, R.H., 1979. Isotopic dating of older elements (including the Cabo Ortegal mafic-ultramafic complex) in the Hercynian orogen of NW Spain: manifestations of a presumed early Palaeozoic mantle-plume. Chemical Geology 24, 35–56.

Van Overmeeren, R.A., 1975. A gravity investigation of the catazonal rock complex at Cabo Ortegal (NW Spain). Tectonophysics 26, 293–307.

Van Zuuren, A., 1969. Structural petrology of an area near Santiago de Compostela (NW Spain). Leidse Geologische Mededelingen 45, 1–71.

Vauchez, A., Nicolas, A., 1991. Mountain building: strike-parallel motion and mantle anisotropy. Tectonophysics 185, 183–201.

Vielzeuf, D., Holloway, J.R., 1988. Experimental determination of the fluid-absent melting relations in the pelitic system. Consequences for crustal differentiation. Contributions to Mineralogy and Petrology 98, 257–276.

Vogel, D.E., 1967. Petrology of eclogite- and pyrigarnite-bearing polymetamorphic rock complex at Cabo Ortegal, NW Spain. Leidse Geologische Mededelingen 40, 121–213.

Vogel, D.E., Abdel Monem, A.A., 1971. Radiometric evidence for a Precambrian metamorphic event in NW Spain. Geologie en Mijnbouw 50, 749–750.

Vollmer, F.W., 1988. A computer model for sheath nappes formed during crustal shear in the Western Gneiss Region, central Norwegian Caledonides. Journal of Structural Geology 10, 735–743.

Wilson, G., 1961. Tectonic significance of small-scale structures and their importance to geologists in the field. Annales de la Société Géologique de Belgique 84, 423–548.